

# **Technology and Design Kits for Printed Electronics**



## **Deliverable report**

### **D2.5.U**

## **Report on modeling, variability and validation**

**Dissemination Level: CO**

**Nature of deliverable: R**

Project acronym : **TDK4PE**  
Grant Agreement no: 287682





# **Deliverable D2.5.U**

## **Modeling, variability and validation**

**WP number: WP2**

**Lead Beneficiary number: 4**

**Lead Beneficiary name: IFS**

**Dissemination Level: PU**

**Nature of deliverable: R**

**Delivery Month: M23**

List of authors

Henrique Gomes




Yoann Courant, Philippe Heredia, Firas Mohamed

Carme Martínez Domingo, Eloi Ramon, Jordi Carrabina

Francesc Vila, Jofre Pallares, Lluís Teres

Niels Olij, Arjen Bakker

Creation date:	19/04/2013	Revision:	1.4
Document ref.:	Report on, modeling, variability and validation	Num. of pages:	48

WP Leader: <b>IFS (4)</b>		
Partner in charge <sup>1,2</sup> :	<b>IFS (4)</b>	
Responsible persons <sup>2</sup> :	<b>Firas Mohamed, Yoann Courant, Ph. Heredia</b>	
Contributing partners		
Partner <sup>2,3</sup> :	<b>UAB (1)</b>	
Persons <sup>2</sup> :	<b>Jordi Carrabina, Carme Martínez, Eloi Ramon, Gerard Sisó, Paris Vélez</b>	
Partner <sup>2,3</sup> :	<b>UAlg (9)</b>	
Persons <sup>2</sup> :	<b>Henrique Gomes</b>	

Rev.	Date	Authors / Reviewers	Remarks
1.3	08/11/2013	F. Mohammed	Sections 8 & 9
1.2	05/11/2013	H. Gomes	Review of diode and OTFT models and extraction procedures
1.1	30/10/2013	F. Mohammed	Review & add sections
1.0	21/10/2013	J. Carrabina	Restructuring D2.3.U & D2.5.U

<sup>1</sup> Partner/Person(s) responsible(s) of this delivery.

<sup>2</sup> Specify: Partner SHORT-NAME (partner #).

## Contents

<b>Contents .....</b>	<b>2</b>
<b>List of Figures.....</b>	<b>4</b>
<b>List of Tables .....</b>	<b>5</b>
<b>List of Acronyms.....</b>	<b>5</b>
<b>Summary .....</b>	<b>6</b>
<b>Applicable Documents .....</b>	<b>6</b>
<b>1 MODELING.....</b>	<b>7</b>
1.1 Physical modeling .....	7
1.2 Behavioral modeling .....	7
1.3 Semi-physical modeling .....	8
1.4 Complete story.....	9
<b>2 Parameter extraction for electrical characterization .....</b>	<b>11</b>
2.1 Test vehicles for parameter extraction .....	11
<b>3 Device models and parameters .....</b>	<b>13</b>
3.1 Resistor model .....	13
3.1.1 Parameter extraction procedure.....	14
3.2 Capacitors model .....	15
3.2.1 Parameter extraction procedure.....	16
3.3 Inductor models .....	18
3.3.1 Parameter extraction procedure.....	19
3.4 RF devices and transmission line models .....	21
3.4.1 Parameter extraction procedure.....	21
3.5 Shottky Diode model .....	25
3.5.1 Parameter extraction procedure.....	26
3.6 Organic Thin Film Transistors (OTFTs) models.....	28
3.6.1 Parameter extraction procedure.....	28
<b>4 Designing experiments by Input Sampler.....</b>	<b>31</b>
4.1 Introduction.....	31
4.2 Optimal experiment design .....	31
4.3 Generating new experiments .....	31
4.4 Modeling trial of the horizontal linear resistor LR01 .....	32
<b>5 Validation .....</b>	<b>34</b>
5.1 Blind validation .....	34
5.2 Viewing models behavior .....	35
5.3 Validation based on new printed samples .....	35
<b>6 Model validity .....</b>	<b>36</b>
6.1 Models export .....	36
<b>7 Dynamic modeling.....</b>	<b>37</b>
<b>8 Variability.....</b>	<b>38</b>
8.1 Variability Management .....	38
8.1.1 Variability management on mathematical models .....	38
8.1.2 Variability management on physical models .....	39
8.2 Strategy to cope with variability and yield .....	40
8.2.1 One model per transistor dimension .....	40
8.2.2 General model for OTFTs .....	41
8.3 Variability analysis.....	41

8.3.1 Preliminary example of the application of the UMEM model to simulates I-V characteristics of OTFTs produced within the TDK4PE consortium.....	41
<b>9 Methodology proposed inside TDK4PE.....</b>	<b>43</b>
<b>9.1 Integrated models .....</b>	<b>43</b>
9.1.1 Infiniscale Semi-physical model .....	43
9.1.2 UCM Semi-physical model .....	44
<b>9.2 Example Devices .....</b>	<b>44</b>
9.2.1 Load and Drive OTFTs .....	44
<b>9.3 Example Circuits .....</b>	<b>45</b>
9.3.1 Inverters and Ring Oscillator .....	45
<b>10 Conclusions .....</b>	<b>47</b>
<b>11 References .....</b>	<b>48</b>
<b>11.1 Documents.....</b>	<b>48</b>

## List of Figures

Figure 1: Physical modeling. ....	7
Figure 2: Behavioral modeling.....	8
Figure 3: Semi-physical modeling.....	9
Figure 4: Modeling complete flow. ....	9
Figure 5. Schematic diagram of the characterization vehicles and parameter extraction in the development and qualification of the technology. ....	12
Figure 6. Schematic structure of the different layers used to make MIS capacitors or TFT devices. ....	13
Figure 7. Physical parameters used to estimate the resistance of a material.....	14
Figure 8. (a) Photograph of a linear resistor, (b) schematic arrangement of the layer layout. ....	14
Figure 9. Layout structure of a printed capacitor.....	16
Figure 10. Equivalent circuit for a MIM structure.....	16
Figure 11. Typical spiral inductor topologies (square, hexagonal, octagonal and circular). Extracted from [5] .....	18
Figure 12. Electrical model of an inductor. ....	19
Figure 13. Typical inductor frequency response: Impedance absolute value and phase (a) and inductance frequency response (b). Extracted from [6] .....	20
Figure 14. Microstrip ring resonator. Bottom ground plane not represented. ....	22
Figure 15. Typical S-parameters response of a band-pass filter. $S_{21}$ represents transmission or gain and $S_{11}$ is the reflection loss (in dB) .....	23
Figure 16. TRL differential calibration kit (left) and devices under test PCB (right). Extracted from [9] .....	24
Figure 17. Rectifying I-V curve.....	25
Figure 18. Energy barrier at the interface between a n-type semiconductor and a metal. ....	25
Figure 19. Schottky diode structure: (a) cross section and (b) top view.....	26
Figure 20: Incremental input sampler. ....	31
Figure 21: Modeling ENEA OTFT .....	32
Figure 22: Semi-Physical modeling of OTFTs data.....	32
Figure 23: Variability curves for LR01_A_130405_01_D-UAB_130423 .....	33
Figure 24: Variability curves for LR02_130321_01_A_D-UAB .....	33
Figure 25: Semi-Physical modeling of OTFTs data.....	34
Figure 26: Error report on modeling and validation data. ....	35
Figure 27: Managing Variability by MIN/MAX modeling. ....	38
Figure 28: Monte Carlo sampling. ....	40
Figure 29: Transfer curve measured in the liner region ( $V_{DS} = -1V$ ) .....	42

Figure 30: Comparison between experimental (dotted line) and simulated (full line) I-V characteristics using the UMEM model .....	42
Figure 31: Managing variability within the consortium .....	43
Figure 32: New semi-physical GUI .....	44
Figure 33: Load OTFT: ID-vs-VD and Load OTFT ID vs VG .....	45
Figure 34: Drive OTFT modeling: ID vs VD and ID vs VG .....	45
Figure 35: simulated inverter transfer curve based on semi-physical models.....	46

## List of Tables

Table 1- Summary of the electrical test vehicle and parameter extraction for capacitors	18
Table 2- Summary the electrical test vehicle and parameter extraction for inductors.....	21
Table 3. Summary the electrical test vehicle and parameter extraction for inductors .....	24
Table 5. Experimental OFET parameters and measurement procedures. ....	30
Table 6. TFT parameters extracted from the simulation of the output <i>I-V</i> curves .....	42

## List of Acronyms

TDK4PE	<b>Technology Design Kit for Printed Electronics</b>
PU	<b>Dissemination level Public</b>
PP	<b>Dissemination level Restricted to other programmed participants (including the Commission Services).</b>
RE	<b>Dissemination level Restricted to a group specified by the consortium (including the Commission Services)</b>
CO	<b>Dissemination level Confidential, only for members of the consortium (including the Commission Services)</b>
R	<b>Nature of the deliverable Report</b>
P	<b>Nature of the deliverable Prototype</b>
D	<b>Nature of the deliverable Demonstrator</b>
O	<b>Nature of the deliverable Other</b>



## Summary

TDK4PE relies in the successful fabrication of organic based circuits using inkjet printed materials. These circuits use thin film transistors (TFTs), diodes and resistors as basic build blocks. The performance of these devices is essentially controlled by intrinsic material parameters (such as carrier mobility, free carrier concentration), and by extrinsic parameters, among these the most important one is the density of electrical active impurities present at interfaces. For TFTs the most relevant interface is the dielectric/semiconductor interface, while for diodes and resistors the metal/semiconductor interface is critical. This report provides an account of the parameters (and appropriate techniques) to be measured/extracted according to the electrical device models. The measurements proposed should provide feedback information for adjustment of the fabrication process and in this case the speed of the measurement is crucial. This task will be undertaken on a phenomenological basis, relying on experience and statistical correlations, this is justified because the understanding of fundamental relationships between cause and effect is still lacking.

Understanding that variability and yield are key issues for building circuits out of a large number of devices lets us to consider the variability issues at circuit simulation level that have to agree with the results of model parameters extraction.

Finally it is presented a technology to design experiments called InputSampler.

As a summary this report:

- a) Specifies the models to be used and the parameters to be extracted.
- b) Defines techniques and measurement protocols suitable for all inkjet organic based electronics (low mobility, poor environmental stability, drifts). The objective is to minimize data dispersion caused by inadequate measurement procedures.
- c) Specifies the devices modelling and validation procedure.
- d) Proposes a two phase strategy to cope with circuit simulation according to the selection and usage of limited number of transistors sizes.

## Applicable Documents

List of previous project reports needed or useful to understand this one, in chronological order:

1. Deliverable D2.3: TDK Development Guide: Cell Library Development and Characterization.
2. Deliverable D6.1: TDK Multi-Printing Process organization and schedule.

# 1 MODELING

This section describes the modeling techniques going from physical to behavioral modeling.

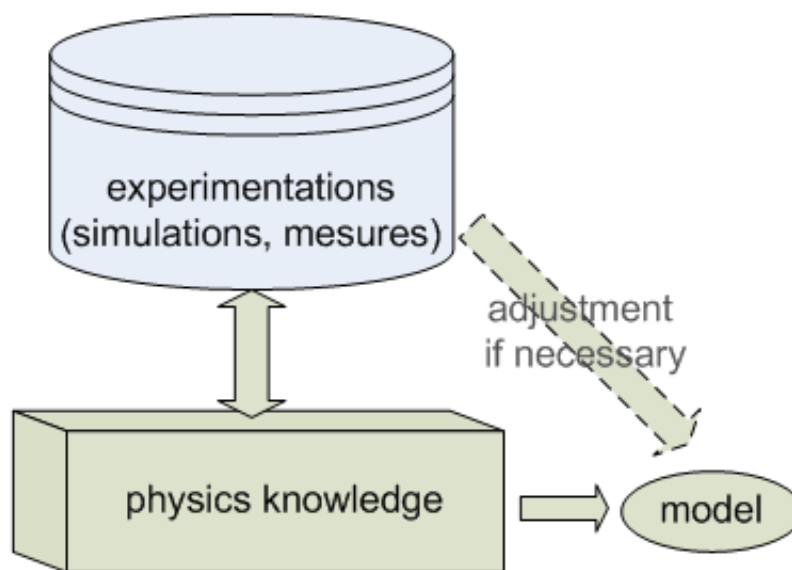
The goal of is to clarify the concepts and procedures concerning Modeling, Validation and Variability Management for the devices built inside the TDK4PE project, especially for Organic Thin Film Transistors.

This clarification is needed due to the different understanding that we noticed among the different communities involved in the project, basically the organic and the silicon ones.

Once these main goals are clarified, a proposal will be made for managing in the project, the whole process from device fabrication to circuit simulation using those devices.

## 1.1 Physical modeling

Physical modeling consists in elaborating physical model based on physics knowledge and adjusting them if necessary from experiment measures. Figure 1 describes this framework.



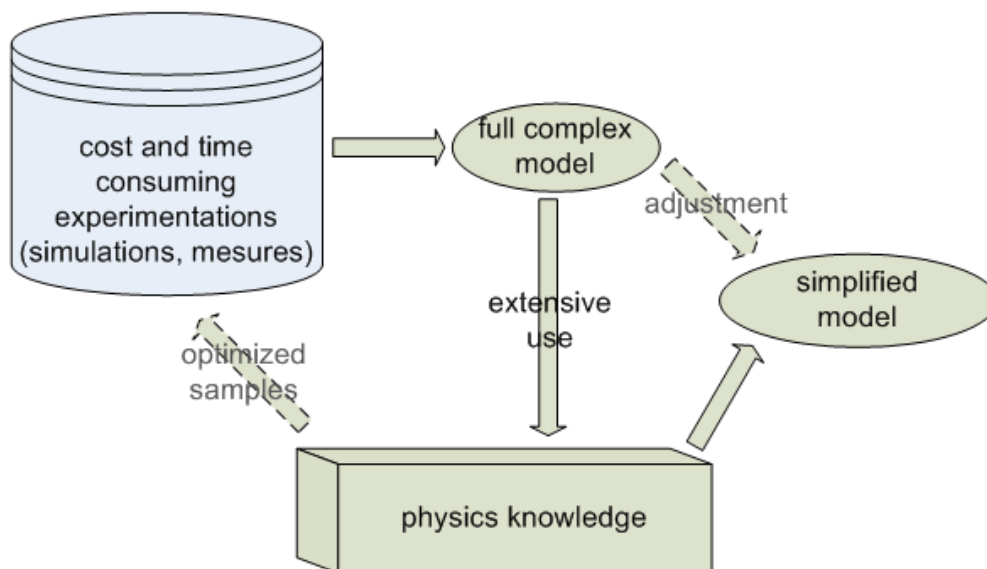
**Figure 1: Physical modeling.**

One main advantage of this approach is to have a physically certified model. Nevertheless the cost of this advantage is a coarse-grain simplification of the model that could become far away from real complex phenomena.

## 1.2 Behavioral modeling

Face to time and cost consuming experimentations, behavioral modeling proposes to model the physical phenomena from a mathematical point of view. These models are often called black-box models because their comportement is complex and also often directly intractable from a human analysis.

Their own benefit is to tackle whole phenomena<sup>3</sup> by replacing time consuming and costly experimentation with fast evaluation of models<sup>4</sup>. Figure 2 shows this kind of modeling. These models are grounded on mathematical formulation. Nevertheless they can help to analyze whole physical phenomena and to build simplified (but physically inspired) models. For example these simplified models could handle phenomena only in specific zone of data, or only some aspect of phenomena.



**Figure 2: Behavioral modeling.**

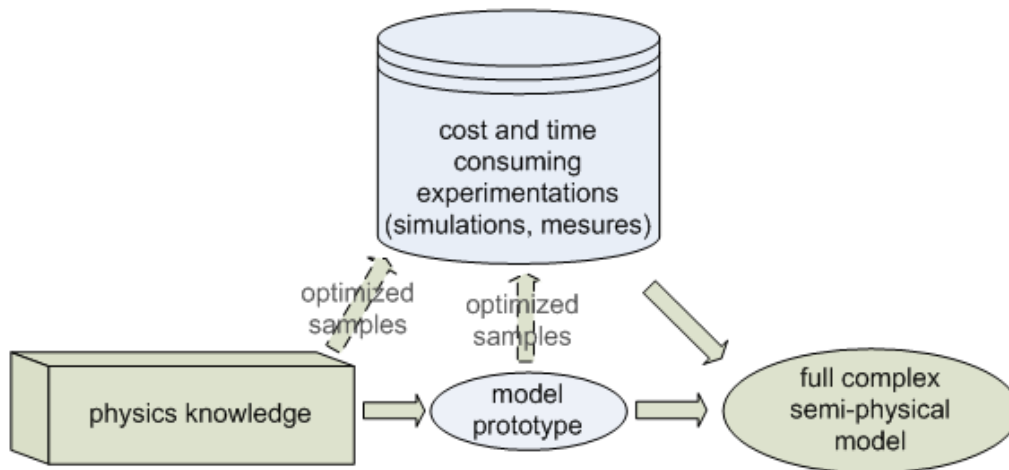
### 1.3 Semi-physical modeling

To combine the advantages of physical modeling and behavioral modeling, semi-physical modeling propose to design a physical model prototype from physics knowledge. This prototype is grounded on physical certified formula and has some indeterminate part such as undefined constant (as generally in physical modeling) but also undetermined function of some variable<sup>5</sup>. Then some behavioral modeling technique could be adapted to handle the physical model prototype instead of a mathematical model that could be incompatible with physics knowledge. The model is often compared as a gray-box: some physical aspects of the model are visible and tractable, other are handled by mathematics formula that could be physically erroneous. Very soon, the modeler will be able to treat semi-physical modeling.

<sup>3</sup> to be more exact the model is defined with a confidence interval and is only an approximation of phenomena

<sup>4</sup> this suppose that the model has lower cost than experimentation which it's generally the case.

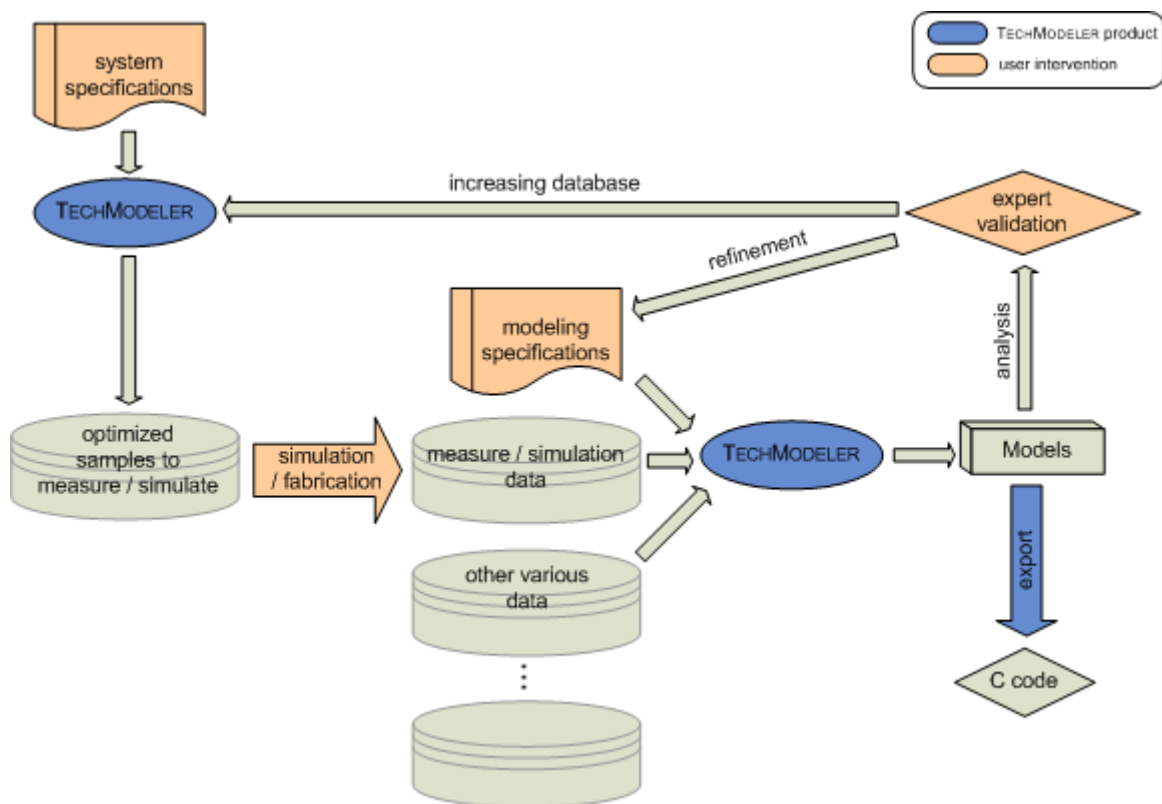
<sup>5</sup> In a way semi-physical modeling can be viewed as a generalization of physical modeling



**Figure 3: Semi-physical modeling.**

### 1.4 Complete story

Needed data for sampling can be optimized. An advanced technology called "Optimal experiment design" has been developed to generate samples in multi-dimension space. Samples are chosen in a way to cover the input space of parameters while removing redundancy, i.e. avoiding samples that do not bring more information, for example those that are too close from initial samples. The flow can be detailed as in Figure 4.



**Figure 4: Modeling complete flow.**

First the user describes the physical system and then creates an optimized database. After simulation or fabrication and measures of the samples, the user defines modeling specifications to create models. The models can be refine by changing modeling specifications

## 2 Parameter extraction for electrical characterization

In this section, we will discuss the need off electrical parameters for the device models a complete technology characterization.

### 2.1 Test vehicles for parameter extraction

Electrical characterization can be carried out in three different samples such as (i) witness samples, (ii) test vehicles and (iii) non specialized final circuits.

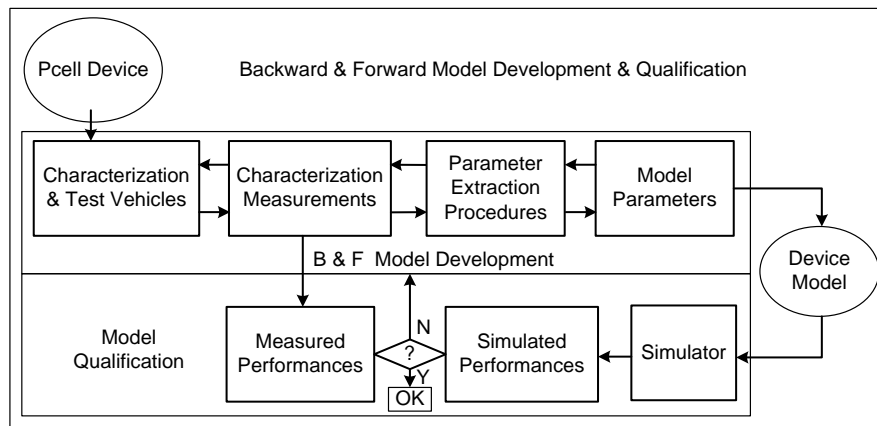
Witness samples are samples without active function. These samples are used to obtain information of a particular manufacturing step. Examples include the morphology or the roughness of a particular layer. However, the interaction of layers varies from batch to batch. In the case of the non-specialized circuits, the sample contains all the processing steps, but the characterization may not be as straightforward as in witness samples. Because of these constraints, test vehicles were specially designed to allow effortlessly the extraction of the device parameters using electrical techniques. Simulation programs such as SPICE, employ devices models (BSIM3, BSIM4 –more information in D2.3-) for circuit simulation, which uses electrical (and physical) parameters.

In this section we will focus on the test vehicles designed to be probed using electrical measurements. The electrical characterization includes both DC or quasi-static techniques such as current-voltage measurements ( $I$ - $V$ ) and small signal (AC) impedance based techniques such as capacitance-voltage ( $C$ - $V$ ) profiling. A detailed description of test equipment used for this characterization in each TDK4PE node is listed in D6.1.

Regarding the physical-based models for circuit simulation, two main classes of parameters are taken into account, electrical and geometrical parameters. For instance, concerning the drain current in linear regime equation of an OTFT, as shown equation 1, the electrical parameters are the mobility ( $\mu$ ), insulator capacitance ( $C_i$ ) and the threshold voltage ( $V_T$ ); the geometrical parameters are the length ( $L$ ) and width ( $W$ ), and the  $V_{GS}$  and  $V_{DS}$  are the electrical test parameters. The electrical characterization of the test vehicle allows the electrical parameters extraction and to obtain the values of the device model.

$$I_{DS} = \frac{W}{L} \mu_{lin} C_i V_{GS} - V_T V_{DS} \quad (1)$$

The basic role of electrical characterization in the technology is shown in Figure 5. In order to find the parameters value for a device, according to a specific device model, different characterization procedures are required. A good fitting between the model and the parameters occurs when the simulation and the real measurements matches.

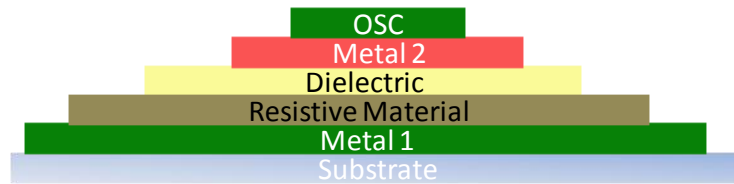


**Figure 5. Schematic diagram of the characterization vehicles and parameter extraction in the development and qualification of the technology.**

### 3 Device models and parameters

In this section we will focus on the models and parameters to be extracted for linear and snake resistors, capacitors, inductors, diodes and OTFTs.

The devices are function of the material stack arrangement because of the interaction among them is important. Regarding TDK4PE technology, which is based on PMOS technology, the material stack is shown in Figure 6. It is worth to note that this order of the materials leads to the Bottom Gate Bottom Contact OTFT structure.



**Figure 6. Schematic structure of the different layers used to make MIS capacitors or TFT devices.**

#### 3.1 Resistor model

The most elementary of all devices is the resistor. It consists of a bar of homogeneous materials with two contacts at the extremes. Injection of carriers is assumed to be unhindered and the current only limited by the resistivity of the material. The electrical parameter of a resistor is its resistance  $R$  of the material, which is defined by Ohm's Law (equation 2):

$$R = \frac{V}{I} \quad (2)$$

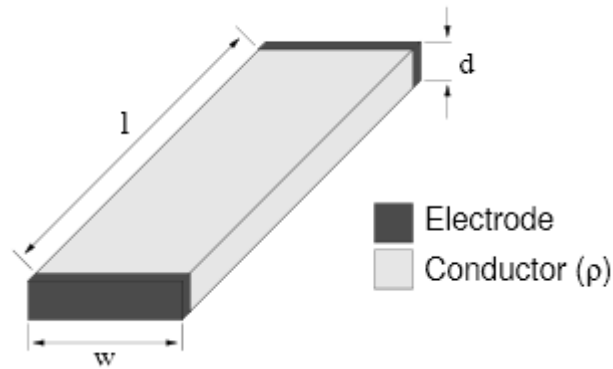
The reciprocal of this resistance is called conductance  $G$  and is a more adequate entity in electrical characterization. Both device parameters resistance (equation 3) and conductance (equation 4) can be expressed in their material parameters, resistivity  $\rho$  and conductivity  $\sigma$ , according to

$$R = \rho \frac{d}{A} \quad (3)$$

$$G = \sigma \frac{A}{d} \quad (4)$$

where  $A$  is the cross-section area and  $d$  the length of the device (Figure 7).

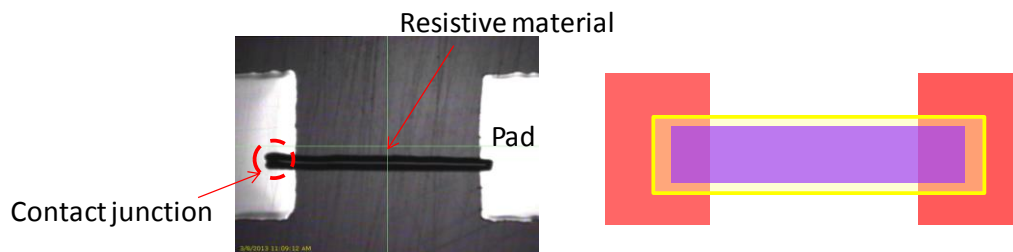




**Figure 7. Physical parameters used to estimate the resistance of a material.**


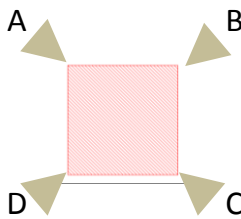
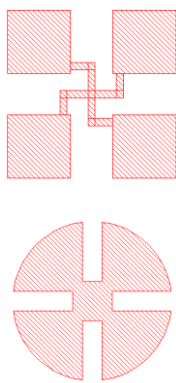
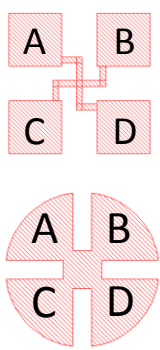
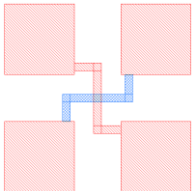
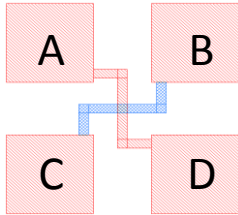
However the Ohm's Law and if we consider the whole resistor device, a parasitic series resistance is created at the junction of the resistive material and the pads due to the difference in their work functions. This parasitic resistance is called Contact Resistance,  $R_{contact}$ , and it has an Ohmic contact behavior. Then, the resistance of the resistor device is composited by the material and the contacts (equation 5). The following expression is used to model the device, having two areas of interfacial contact as shown in Figure 8.

$$R = R_{material} + 2R_{contact} \quad (5)$$



**Figure 8. (a) Photograph of a linear resistor, (b) schematic arrangement of the layer layout.**

### 3.1.1 Parameter extraction procedure

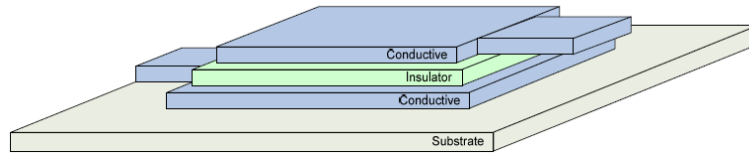
Parameters extracted	Test vehicle	Test vehicle layout	Characterization measurements	Characterization procedure
Rs <sub>sheet</sub> Resistivity	<b>Van Der Pauw</b>		 Contacts in the extremes	Four- probe measurement. Apply a curve from 0v to 1-2v between A & B contacts, and measure current (I) between C & D contacts.
Rs <sub>sheet</sub> Resistivity Linewidth	<b>Greek cross</b>		 Contacts on the pads	Four- probe measurement. Apply a curve from 0v to 1-2v between A & B contacts, and measure current (I) between C & D contacts.
R <sub>contact</sub>	<b>Greek cross for R<sub>contact</sub></b>	Material 1 (Blue pattern) and Material 2 (Red pattern) 	 Contacts on the pads	Four- probe measurement. Apply a curve from 0v to 1-2v between A & B contacts, and measure current (I) between C & D contacts.

### 3.2 Capacitors model

The capacitor is a component which has the ability or "capacity" to store energy in the form of an electrical charge producing a potential difference across its plates. In its basic form, capacitors consist of two parallel conductive (metal) plates which are not connected or touching each other, but are electrically separated either by air or by some form of insulating material commonly called the capacitors dielectric. Capacitance measures how well the charge is stored.

The conductive metal plates of a capacitor can be square, circular or rectangular, or they can be a cylindrical or spherical shape. In printing technology, the capacitors are planar

as shown in Figure 9. This structure is known also as Metal-Insulator-Metal (MIM) sandwich structure.



**Figure 9. Layout structure of a printed capacitor**

The capacitance of parallel plate capacitor is proportional to the area  $A$  and inversely proportional to their distance  $d$  (i.e. the dielectric thickness) and it is expressed in the equation (10).

$$C = \frac{\epsilon_0 \epsilon_r \cdot A}{d} \quad (6)$$

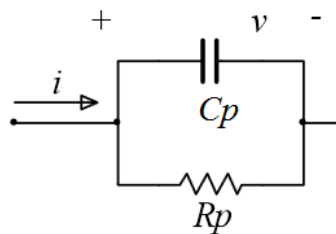
Where  $\epsilon_0$  is the permittivity of the vacuum and  $\epsilon_r$  is the dielectric constant.

The parameters such dielectric constant, capacitance, thickness of the dielectric, area, resistance and losses of the capacitors can be extracted by test vehicles.

### 3.2.1 Parameter extraction procedure

The electrical test vehicle for the assessment of dielectric is the MIM structure, as show Figure 9.

Since the dielectrics are used in the gate of the TFT (Thin-Film Transistors), the study of the leakage current and resistivity is of paramount importance. The dielectric material between the plates of a capacitor has a finite resistivity (compared to infinite resistance of an ideal capacitor) then, a small amount of current could flow through the capacitor. The real capacitor is modeled as a capacitor and resistor in parallel as shown in Figure 10.



**Figure 10. Equivalent circuit for a MIM structure.**

The electrical test applied to the MIM test vehicle is based on the Admittance spectroscopy. Admittance spectroscopy is a technique that consists of applying a bias

and a small-signal voltage, at a radial frequency ( $\omega=2.\pi.f$ ). The response to this probe signal is a current composed of an AC and DC part. When the admittance of the MIM test structure is measured, this admittance can be translated into a parallel capacitance and resistance (or loss) whose values  $C_p$ ,  $R_p$ , depend on the radial frequency.

In the case of capacitor, the current is fully 90° out-of-phase with the voltage. A useful parameter is loss  $L$ . This has the same unit as capacitance, namely farad, and is defined as the conductance divided by the radial frequency as show equation 11.

$$L = \frac{G}{\omega} \quad (7)$$

Where  $G$  is  $I_{AC} / V_{AC}$ . Loss is therefore, like conductance, in-phase with the voltage. Finally the loss-tangent is defined as the real part of admittance divided by the imaginary part, and is therefore a dimensionless entity. It can be understood that the loss-tangent is also the ratio of loss and capacitance as shown equation 12.

$$\tan \delta = \frac{L}{C} = \frac{1}{\omega R_p C_p} \quad (8)$$

The parameter  $\delta$  shows how "lossy" is the dielectric and thus the capacitor, and ideal capacitor has  $\delta=0$ . However, an ideal conductor does not store charge and  $\delta$  has a value of 90°.

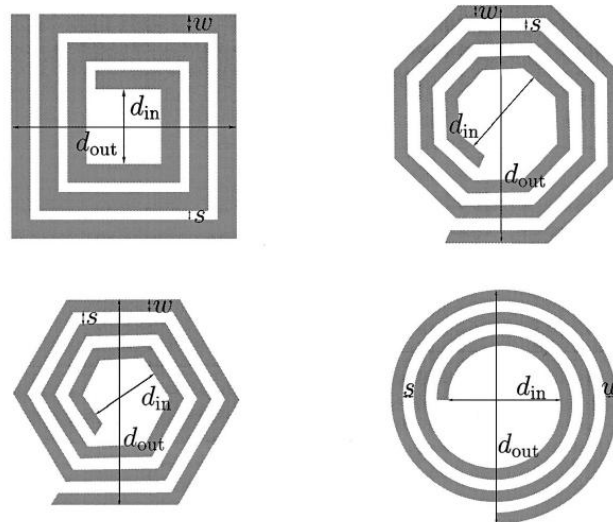
To extract the  $R_p$  and  $C_p$ , the electrical test is based on applying an AC signal of 100 mV at 1kHz using two-points measurement performed using a LCR meter or Impedance analyzer. The dielectric permittivity can be calculated by the equation 9 when  $A$  and  $d$  are already known. The variation of the admittance can be evaluated in function of the frequency, for this case a sweep of frequency is performed during the measurement of the  $R_p$  and  $C_p$ . As the frequency increase, the capacitance decreases since they are inversely proportional. It means that for high operation frequency of the circuits, the dielectric will behave leakier. Table 1 shows a summary of the electrical test vehicles and its parameter extraction.

Model parameter	Parameter extraction procedures	Characterization measurements	Characterization equipment	Test vehicle
<b><math>R_p</math> and <math>C_p</math> at a certain frequency</b>	Use a test frequency of 1 kHz, AC signal 100mV	2 points-measurement Measure $C_p$ and $R_p$	LCR meter, Impedance Analyzer	MIM
<b>Loss Capacitance and <math>\tan \delta</math> in function of frequency</b>	Use a sweep test frequency from 20Hz up to MHz, AC signal 100mV	2 points-measurement Measure $C_p$ and $R_p$	LCR meter, Impedance Analyzer	MIM

**Table 1- Summary of the electrical test vehicle and parameter extraction for capacitors**

### 3.3 Inductor models

An inductor is a passive component that stores energy in form of magnetic field. It consists on a wire or other conductor wound into a coil (this coil can be air). The inductance is a property by which a variation of the current produces a varying magnetic field that induces voltage in the conductor (inductor) itself and/or other conductors nearby. For RF applications a typical implementation is a printed spiral on the substrate. Several topologies can be used, as is shown in Figure 11.



**Figure 11. Typical spiral inductor topologies (square, hexagonal, octagonal and circular).  
Extracted from [5]**

Inductance must be calculated in function of the used implementation. For planar spiral inductances, expressions introduced in [5] are typically used:

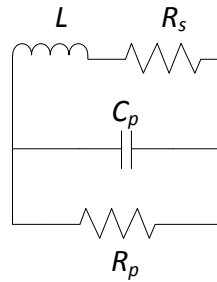
$$L_{mw} = K_1 \mu_0 \frac{n^2 d_{avg}}{1 + K_2 \rho} \quad (9)$$

$$L_{gmd} = \frac{\mu n^2 d_{avg} c_1}{2} \ln c_2 \rho + c_3 \rho + c_4 \rho^2 \quad (10)$$

The first approximation ( $L_{mw}$ ) is based on a modification of an expression developed by Wheeler; the second ( $L_{gmd}$ ) is derived from electromagnetic principles by approximating the sides of the spirals as current-sheets. In these expressions,  $\mu_0$  is the vacuum permeability,  $d_{avg}$  is the average diameter of the spiral  $d_{avg} = 0.5 (d_{out} + d_{in})$  and  $\rho$  is the fill ratio  $\rho = \frac{d_{out} - d_{in}}{d_{out} + d_{in}}$ .  $K_i$  and  $c_i$  are topology depending coefficients. Tables are given in [5].

### 3.3.1 Parameter extraction procedure

A printed spiral inductor can be modeled as shown in Figure 12.



**Figure 12. Electrical model of an inductor.**

$R_s$  represents the metal loss (resistance of the conductor),  $R_p$  is the coil loss and  $C_p$  is the distributed capacitance between the turns of the conductor. In the considered structures,  $R_p$  can be neglected because  $L$  is small and the capacitance between the turns dominates over these losses.

Using a LCR meter is possible to extract the inductor parameters. Measuring in  $L_s$ - $R_s$  mode,  $L_s$  value can be expressed as:

$$L_s = \frac{X}{\omega} = \frac{L}{1 - \omega^2 L C_p - \frac{C_p R_s^2}{L}} \quad (11)$$

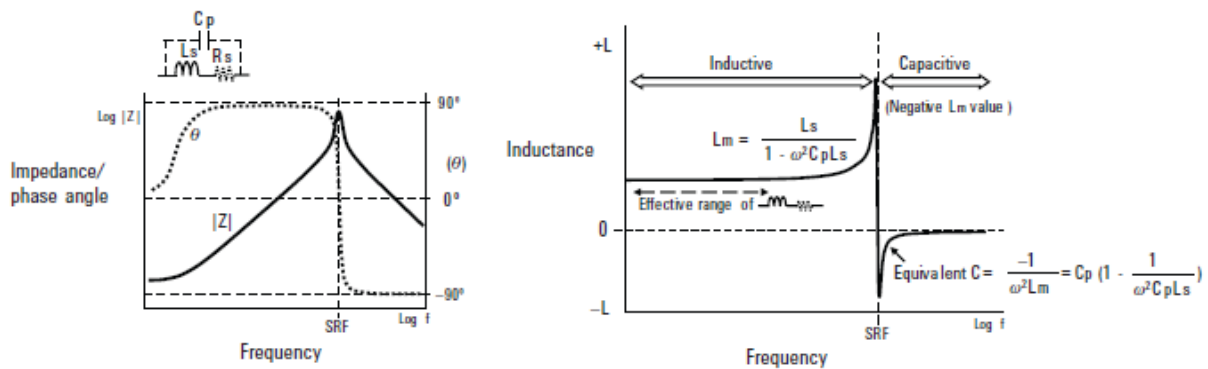
If  $\omega^2 C_p^2 R_s^2 \ll 1$  and  $\frac{C_p R_s^2}{L} \ll 1$ , is possible to simplify  $L_s$ :

$$L_s \cong \frac{L}{1 - \omega^2 L C_p} \quad (12)$$

The stray capacitance  $C_p$  determines the self-resonant frequency (SRF) of the inductor. At SRF, the inductor presents maximum impedance. At frequencies above SRF,  $C_p$  is dominant and inductor exhibits a capacitive behavior (Fig. 18).

Quality factor can be obtained from  $L_s$ - $R_s$  characterization since:

$$Q = \frac{2\pi f L_s}{R_s} \quad (13)$$



**Figure 13. Typical inductor frequency response: Impedance absolute value and phase (a) and inductance frequency response (b). Extracted from [6]**

As can be seen in Figure 13 (b), the measured inductance ( $L_m$ ) takes its maximum value at SRF.

Using LCR meter is possible the characterization of inductors up to 2 MHz. A vector network analyzer can be used for measurements at higher frequencies. In this case we can obtain S-parameters of the inductor under test and inductor parameters can be extracted from measured impedances using commercial circuit simulation tools, such as *Agilent Advanced Design System*. Real part of input impedance gives us the series resistance value ( $R_s$ ), and from imaginary part we obtain the reactance. Taking these values at low frequencies, stray capacitance ( $C_p$ ) is negligible and inductance ( $L$ ) can be obtained from reactance.

Measuring at higher frequencies allows also obtaining SRF, typically higher than 2 MHz for the characterized inductors, and, from this frequency,  $C_p$  can be obtained:

$$\omega_{SRF} = \frac{1}{L C_p} \quad (14)$$

Table 4 shows a summary of the electrical test vehicles and its parameter extraction.

Model parameter	Parameter extraction procedures	Characterization measurements	Characterization equipment	Test vehicle
$L_s - R_s$ $Q = \omega L_s / R_s$	Use a sweep test frequency from 20Hz up to 2 MHz, AC signal 1V	2 points-measurement Measure $L_s - R_s$	LCR meter, Impedance Analyzer	Spiral Inductors
$L_s - R_s - C_p$ $Q = \omega L_s / R_s$ <b>SRF</b>	Use a sweep test frequency from 10 MHz up to GHz.  Extract inductor parameters from S-parameters using software	1 RF port measurement Measure S-parameters	Network Analyzer	Spiral Inductors

**Table 2- Summary the electrical test vehicle and parameter extraction for inductors.**

### 3.4 RF devices and transmission line models

Radiofrequency components, such as filters, couplers, mixers... are an important part in the design of electronic systems. At certain frequencies (from UHF bands) guided wavelengths become shorter and RF devices can be often implemented using planar technology, by means of transmission lines, transmission line sections (stubs) and/or semi-lumped elements. This kind of circuits, usually implemented using conventional PCB techniques, can be also fabricated by means of Printed Electronics.

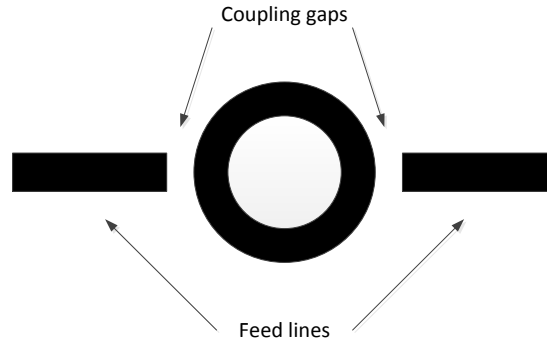
#### 3.4.1 Parameter extraction procedure

For the electrical characterization of the structures, a vector network analyser is typically used for the measure of scattering (S-) parameters. These parameters give information about the electrical properties, such as transmission and reflection characteristics, of the device under test. However, before designing and characterizing RF devices in a given substrate is necessary to know its electrical properties.

#### Substrate electrical characterization

For the design of RF devices using printing electronics techniques, it is necessary the electrical characterization of the substrates. Relative dielectric permittivity ( $\epsilon_r$ ) (dielectric constant) and loss tangent ( $\tan\delta$ ) (dissipation factor) of the substrate can be extracted using several techniques. A simple method is measuring the resonances of a microstrip ring resonator:





**Figure 14. Microstrip ring resonator. Bottom ground plane not represented.**

The distance between feed lines and ring resonator (coupling gaps) must be large in order to avoid variation of the intrinsic resonant frequency of the ring and minimize coupling effects (Figure 14). When the mean circumference of the ring ( $L$ ), is equal to an integral multiple of the guided wavelength, resonance appears:

$$L = 2\pi r = n\lambda_g \quad \text{for } n = 1, 2, 3, \dots \quad (15)$$

Where  $r$  is the mean radius of the ring (difference between inner and outer radius) and  $\lambda_g$  is the guided wavelength, which can be expressed as:

$$\lambda_g = \frac{\lambda_0}{\epsilon_{eff}} = \frac{c}{f_n \epsilon_{eff}} \quad (16)$$

being  $f_n$  the ring resonant frequencies and  $c$  the speed of light in free space.

From equation (19) and (20):

$$\lambda_g = \frac{L}{n} = \frac{2\pi r}{n} \quad (17)$$

From these expressions, it is possible to obtain the effective permittivity, parameter that takes into account that, in a microstrip line, a fraction of electric fields are not constrained within the substrate:

$$\epsilon_{eff} = \frac{nc}{2\pi r f_n}^2 \quad (18)$$

And, finally, from the following empirical expression, the relative permittivity ( $\epsilon_r$ ) can be obtained [7]:

$$\epsilon_{eff} = \frac{\epsilon_r + 1}{2} + \frac{\epsilon_r - 1}{2} \left( 1 + 12 \frac{h}{W} \right)^{-1/2} \quad (19)$$

Where  $h$  is the height of the substrate and  $W$  is the width of the microstrip transmission line. This expression is valid when  $W/h > 1$ , condition satisfied in most cases.

Summarizing, for obtaining the dielectric constant of the substrate at several frequencies we can measure S-parameters of a microstrip ring resonator using a network analyser and obtain the resonant frequencies, where peaks of transmitted power appear, and apply the expressions presented.

In order to obtain the dissipation factor is necessary to calculate the attenuation constant using the following expression:

$$\alpha = \frac{8,686\pi}{Q\lambda_g} \quad (\text{dB/m}) \quad (20)$$

Where  $Q$  is the unloaded quality factor of the ring resonator:

$$Q = \frac{f_n}{f_2 - f_1} \quad (21)$$

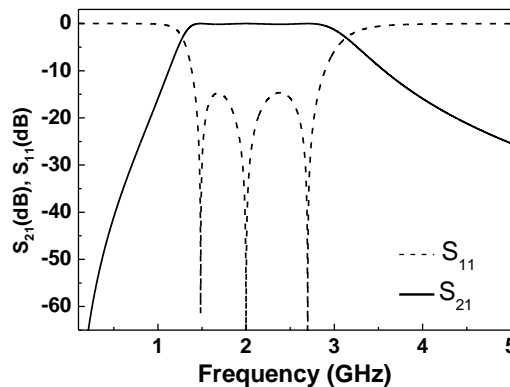
Being  $f_2$  and  $f_1$  the limits of the band (-3dB insertion loss frequencies). The loss tangent ( $\tan\delta$ ) can be obtained from the expression [8]:

$$\alpha = 8.686\pi \frac{\epsilon_{eff}-1}{\epsilon_r-1} \frac{\epsilon_r}{\epsilon_{eff}} \frac{\tan\delta}{\lambda_g} \quad (\text{dB/m}) \quad (22)$$

### Devices electrical characterization

For the electrical characterization of the structures, S-parameters will be measured using a network analyser, in combination with a probe station or using 2.4mm end launch connectors.

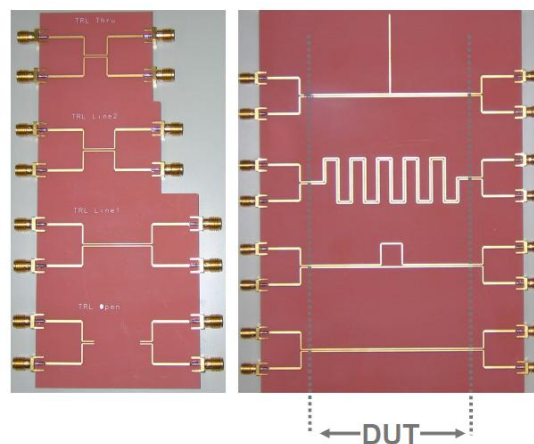
As mentioned before, measuring these parameters we are able to obtain transmission and reflection characteristics of the devices. A typical band pass filter response represented by means of S-parameters is shown in Figure 15.



**Figure 15. Typical S-parameters response of a band-pass filter.  $S_{21}$  represents transmission or gain and  $S_{11}$  is the reflection loss (in dB)**



In order to obtain correct measures, a calibration process must be performed before measuring, with the goal of correcting systematic errors in the instrument, characteristics of the cables and adapters. The most typical calibrations are SOLT and TRL. SOLT (Short-

Open-Load-Thru) is the simplest one and only requires connecting these standards. In some devices is necessary to remove the contribution of connectors and/or transmission lines included in the device under test. Using the same access lines in all the devices is possible to obtain accurate measurements of the designed components by means of de-embedding techniques. De-embedding is a mathematical process that removes the effects of unwanted portions of the structure that are embedded in the measured data by subtracting their contribution. To this end, is necessary to perform TRL (Thru, Reflect, Line) calibration by means of a specifically-designed TRL calibration kit. Figure 16 is an example of a differential TRL kit and devices under test using the same access lines implemented in conventional PCB.



**Figure 16. TRL differential calibration kit (left) and devices under test PCB (right).  
Extracted from [9]**

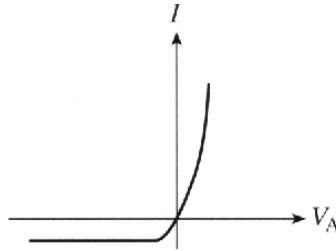
Table 5 shows a summary of the electrical test vehicles and its parameter extraction.

Test vehicle	Test vehicle layout	Characterization measurements	Characterization procedure	Parameters extracted
<b>Printed Microstrip Ring Resonator (substrate characterization)</b>		2 RF ports measurement Network Analyzer	Frequency from 10 MHz up to GHz  Measure S-parameters → Extract ring resonant frequencies and bandwidths → Process data using equations	$\epsilon_r - \tan\delta$ at several frequencies
<b>TRL calibration kit for de-embedding (device characterization)</b>		TRL calibration Network Analyzer	TRL calibration in combination with de-embedding techniques	Corrected S-parameters

**Table 3. Summary the electrical test vehicle and parameter extraction for inductors**

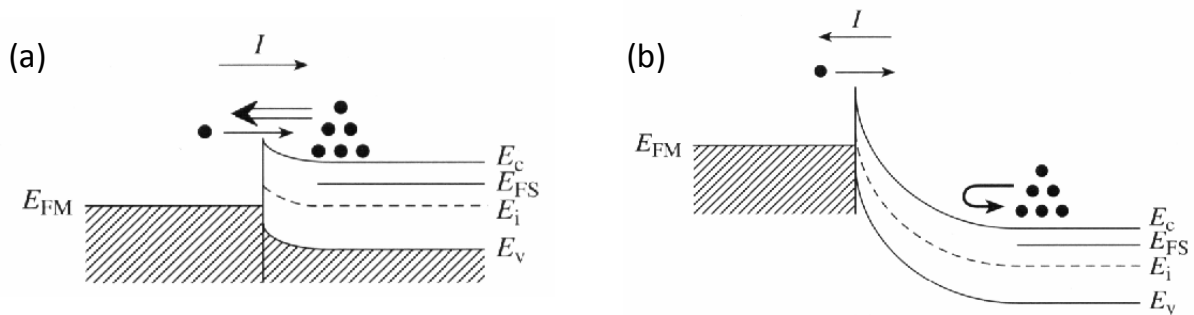
### 3.5 Schottky Diode model

The Schottky diode (shown in Figure 19) consists of a Schottky barrier and, in series, a purely resistive layer. The result is a rectifying element with current in one polarity ("forward") of the bias much larger than in the other polarity ("reverse") as shown in Figure 17. Because of this asymmetry, the electrodes can be distinguished and are called anode and cathode, where the anode is the one that has positive bias in forward polarity.



**Figure 17. Rectifying I-V curve.**

A Schottky barrier is created from the contact of a metal and a semiconductor. Figure 18 shows the space-energy diagram of a metal-n-type semiconductor junction structure and its operation under forward and reverse bias.



**Figure 18. Energy barrier at the interface between a n-type semiconductor and a metal.**

Under forward bias, majority-carrier diffusion from the semiconductor into the metal dominates (Figure 18a). Under reverse bias, majority-carrier diffusion from the metal into the semiconductor dominates which leads to small current (Figure 18b) leading to rectifying behavior.

The current across a metal-semiconductor is mainly due to majority carriers. Three distinctly different mechanisms exist: diffusion of carriers from the semiconductor into the metal, thermionic emission of carriers across the Schottky barrier and quantum-mechanical tunneling through the barrier. The general expression of the current for Schottky diodes is valid for the thermionic field emission and field emission conduction regimes, equation 27.

$$J = J_0 [\exp \frac{qV}{nkT} - 1] \quad (23)$$

with

$$J_0 = AT^2 \exp\left(\frac{-q\Phi_{BP}}{kT}\right) \quad (24)$$

in the thermionic emission conduction regime ( $V > 3 kT/q$ ).

where  $I_0$  is the reverse-bias saturation current,  $A$  is the effective Richardson constant,  $q$  is the electronic charge,  $v$  is the velocity,  $n$  is the ideality factor of a diode, and  $kT$  is 26mV and is known as the thermal voltage. The ideality factor is usually  $\geq 1$  and it parameterizes the deviation from theory. For classic semiconductors such as Si, Ge or GaAs, the value of  $n$  is close to 1, while for polymers it is often in the order of 2. Taking into account the series resistance ( $R_s$ ) of the resistive layer, the current for Schottky diodes follows the equation 29.

$$I = I_0 [\exp(q(V - I \cdot R_s) / nkT) - 1] \quad (25)$$

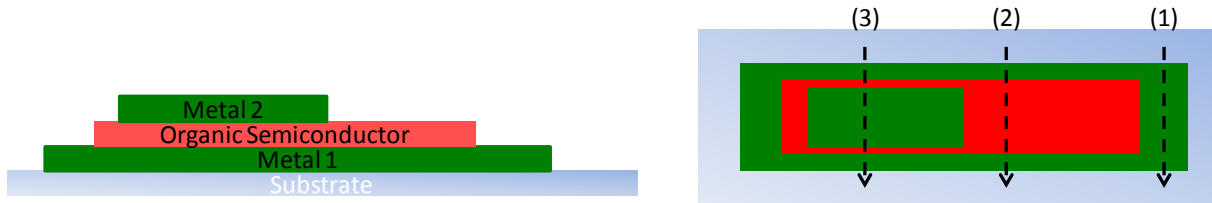
The capacitance of a Schottky barrier can readily be calculated when one realizes that (dynamic) capacitance is defined as the amount of charge that moves in or out of the device when the bias is changed,  $C = dQ/dV$ . The measured (dynamic) capacitance is expressed in equation 30.

$$C/V = A \frac{qNA\epsilon_s}{2V_{bi} - V} \cong A\epsilon_s W \quad (26)$$

$$V_{bi} = \chi + V_n + \Phi_m \quad (27)$$

where  $NA$  is the acceptor density,  $\epsilon_s$  is the dielectric permittivity,  $V_{bi}$  is the bulk-in voltage,  $\chi$  is the electron affinity of the semiconductor,  $qV_n$  is the Fermi level depth relative to the conduction band and  $\Phi_m$  is the workfunction of the metal.

Regarding the equation 30, the Schottky diode behaves like a metal-plates capacitor with electrodes at a distance  $W$  and filled with a dielectric with permittivity  $\epsilon_s$ . Since  $W$  depends on the bias, the capacitance becomes bias-dependent.



**Figure 19. Schottky diode structure: (a) cross section and (b) top view**

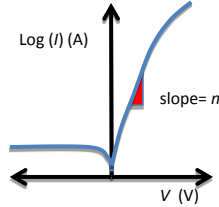
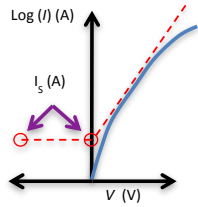
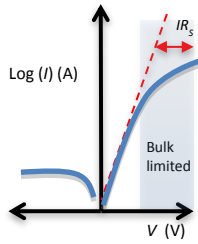
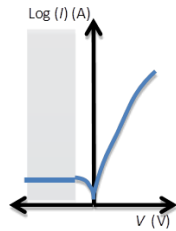
### 3.5.1 Parameter extraction procedure

Metal-Semiconductor structure is the suitable test vehicle for the extraction of the diode parameters. From a DC current-voltage plot ( $\log(I)$ - $V$  plot) we can determine the ideality factor  $n$  from the slope in forward bias and, the saturation current  $I_0$  from the reverse-bias saturation current or the extrapolated-to-zero-volt forward-bias current. Moreover, the rectification ratio of a device ( $r$ ), expressed in equation 32, can be measured. This is an important figure-of-merit since it shows the relative leakage in reverse bias and thus the power efficiency when the device is used in a final circuit.

$$r = I(\text{forward bias}) / I(\text{reverse bias}) \quad (28)$$

To measure the barrier height  $\Phi_{BP}$ , the Schottky diode must be biased into strong reverse bias; the exponent of field emission conduction can be neglected and the slope will be  $-q\Phi_{BP}/k$ . The best way of representing the data is always a form in which they fall on a straight line, it means  $\log(I)$  vs  $V$ .

From an AC Capacitance-Voltage plot we can determine the Built in voltage, the barrier height and the acceptor density. The best way of representing the data is  $C^{-2}$  vs.  $V$  which the form is a straight line. The slope is inversely proportional to the acceptor density  $N_A$  and the interception with the horizontal axis is the  $V_{bi}$ . Table 4 summarizes the parameter extraction, procedure and test vehicle.

Model parameter	Parameter extraction procedures	Characterization measurements	Characterization & tests vehicles
<b>Ideality factor (<math>n</math>)</b>	Forward-bias $I$ - $V$ curve Range: [0 10 V] Voltage ramp speed: 0.1 V/s  Estimate the low-bias linear slope.		<i>Schottky diode</i>  <i>I</i> - $V$ measuring system
<b>Saturation current (<math>I_s</math>)</b>	Saturation current ( $I_s$ ) From the reverse-bias saturation current or the extrapolated-to-zero-volt.		<i>Schottky diode</i>  <i>I</i> - $V$ measuring system
<b>Series resistance (<math>R_s</math>)</b>	For large $V$ : $V = \frac{nkT}{q} \text{Log} \frac{I}{I_s} + IR_s$ $R_s$ is determined from the intercept of the straight line according to the equation $\frac{dV}{d\log(I)} = n \frac{kT}{q} + IR_s$		<i>Schottky diode</i>  <i>I</i> - $V$ measuring system
<b>Barrier height (<math>\phi_{Bp}</math>)</b>	From $I$ - $V$ curve:  For strong bias reverse $V$ :  Estimate the linear slope.		<i>Schottky diode</i>  <i>I</i> - $V$ measuring system
	From $C$ - $V$ curve: Measure the $C$ - $V$ plot at a test frequency of 1 kHz. AC level: 0.1 V.  Once $V_{bi}$ and $N_A$ are known, $\phi_{Bp}$ can be determined: $qV_{bi} = \phi_{Bp} - kT \ln \left( \frac{N_c}{N_A} \right)$		<i>Schottky diode</i>  RCL Meter or an impedance analyzer
<b>Built-in voltage (<math>V_{bi}</math>)</b>	Measure the $C$ - $V$ plot at a test frequency of 1 kHz. AC level: 0.1 V.	Slope $\propto 1/N_A$	<i>Schottky diode</i>

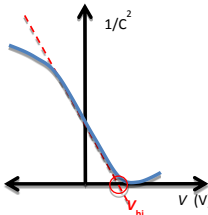
<b>Acceptor density</b> <b>(<math>N_A</math>)</b>	<b>Measurement range:</b> In the reverse bias or low forward bias. Plot the inverse of the junction capacitance against the applied bias. Determine the "flat-band" voltage by a linear extrapolation to the voltage axis.	 $1/C^2 = 2(V_{bi} - V) / A^2 q \epsilon_s N_A$	RCL Meter or an impedance analyzer
<b>Rectification ratio</b>	$I$ (forward)/ $I$ (reverse) measured at $ 5 V$		<i>Schottky diode</i>  $I$ - $V$ measuring system

Table 4- Summary of the electrical test vehicle and parameter extraction for diodes.

### 3.6 Organic Thin Film Transistors (OTFTs) models

The physical model than conveniently describes the OTFT behavior is the Unified Compact Model and parameter Extraction Method (UMEM) developed by A. Cerdeira and M. Estrada [11, 14].

#### 3.6.1 Parameter extraction procedure

The model is a physical based model and allows the extraction of DOS parameters of the organic semiconductor material used in the device. The mobility in OTFTs is based on analytical expressions obtained under the assumption that in all operating range of OTFTs, the concentration of localized charge predominates over free charge. The mobility expression can be written in the form of a power dependence of the gate voltage, allowing the use of the procedure UMEM (Unified model and extraction methodology) to determine all parameters to model the mobility, as well as the electrical characteristics of these transistors. With this method, DOS parameters, considering the typical exponential distribution assumed for OTFTs, can be easily extracted from the transfer characteristic of the device.

In the UMEM model the drain current in the linear region and for  $V_{GS} > V_T$  can be written as

$$I_{DS} = \frac{K}{V_{AA}^\gamma} (V_{GS} - V_T)^{1+\gamma} V_{DS} \quad (28)$$

Or alternatively in the saturation region

$$I_{DS(sat)} = \frac{K}{V_{AA}^\gamma} (V_{GS} - V_T)^{2+\gamma} V_{DS} \quad (29)$$

Where  $V_{AA}$ ,  $K$  and  $\gamma$  are parameters to be extracted.

$$\gamma = 2 \frac{T}{T_0} - 2 \quad (30)$$

$T$  is the absolute temperature and  $T_0$  the characteristic temperature of the DOS

The energy distribution of the DOS  $g_d(E)$ , is expressed as

$$g_d(E) = g_{d0} \exp\left(\frac{E}{K_b T_0}\right) \quad (31)$$

where  $K_b$  is the Boltzmann constant.

$\gamma$  can be extracted from the transfer curves (in the linear region) when plotted as:

$$I_{DS}^{1/(1+\gamma)} \text{ versus } V_{GS} \quad (32)$$

We extract a  $\gamma$  that linearizes the curve. This can be done by trial and error or by an integration procedure as suggested by Cerdeira et al. [14].

For parameter extraction, output characteristics at different values of  $V_{GS}$  as well as transfer characteristics in linear and saturation regimes are need; nevertheless it is suggested to generate the transfer characteristics from the output ones, so data can effectively match.

The field effect mobility ( $\mu_{FET}$ ) is assumed to be in the form

$$\mu_{FET} = \mu_{FET0} (V_{GS} - V_T)^\gamma \quad (33)$$

Table 5 summarizes all the parameters to be extracted together with recommend procedures.

One parameter, the so call contact resistance ( $R_C$ ) deserves some attention. Due to the presence of contacts, the self organization process of molecules is disrupted and hence, very small grains and even voids are formed at the contact edges, resulting in a large number of traps which capture the passing carriers and significantly reduce the carrier mobility in the contact region, manifesting as higher contact resistance. Contact resistance can be model by using a non-linear voltage dependent resistance. This parameter is extracted by fitting the  $I$ - $V$  characteristics.



Parameter	Measurement procedure	Comments
<b><math>\gamma</math> (gamma)</b>	Find $\gamma$ required to linearize the transfer curves. Saturation regime must be used. This because most of the TFTs have parasitic contact resistances that distort the linear transfer curve. Data is plotted as $I_{DS}^{1/(2+\gamma)}$ versus $V_{GS}$ A $\gamma$ that linearizes the curve is extracted.	The $\gamma$ parameter is related with the number of immobile charge density. Therefore, is most determined by the fabrication procedures. Does not depend on gate bias-stress. Contamination from environment may change it with time.
<b>Threshold Voltage (<math>V_T</math>)</b>	Measure the transfer curve in saturation region to avoid distortion from parasitic contact resistances. Data is plotted as $I_{DS}^{1/(1+\gamma)}$ versus $V_{GS}$ A $\gamma$ that linearizes the curve is extracted. $V_T$ is defined as the intercept of the linear $I_{DS}^{1/(2+g)}$ versus $V_{GS}$ curve.	The measurements must be carried out in unstressed OTFTs and in dark conditions.
<b>Field effect mobility (<math>\mu_{FET}</math>)</b>	Once $\gamma$ is extracted then mobility is estimated from the equation: $\mu_{FET} = \mu_{FET0}(V_{GS} - V_T)^\gamma$	
<b>Parasitic contact resistance (<math>R_C</math>)</b>	It is a voltage dependent resistance required to fit the $I$ - $V$ curves on the low bias $V_{DS}$ region. It can be obtained by fitting the $I$ - $V$ curves.	It depends essentially on the trap concentration. Therefore, is most determined by the fabrication procedures.
<b>Off-current (<math>I_{OFF}</math>)</b>	Measure $I_{DS}$ in saturation for $V_{GS} = 0$ V	The initial value is mostly determined by the organic semiconductor layer thickness and doping. It may evolve with ageing and gate-bias-stress.
<b>Leakage current across the gate dielectric (<math>I_G</math>)</b>	Measure the gate current at a particular gate voltage ( $V_{GS} = -20$ V)	

**Table 5. Experimental OFET parameters and measurement procedures.**

In addition to these physical parameters listed in Table 9, there is also variability on the geometrical parameters namely on the channel width ( $W$ ), channel length ( $L$ ), and insulator thickness ( $d_{Ins}$ ). Variability on the internal geometric capacitances is also important for OTFT dynamic behavior.

## 4 Designing experiments by Input Sampler

### 4.1 Introduction

INFINISCALE holds a technology to design experiments. This technology aims to explore as optimized as possible the multi-dimensional space of input parameters with a sphere filling-like algorithm.

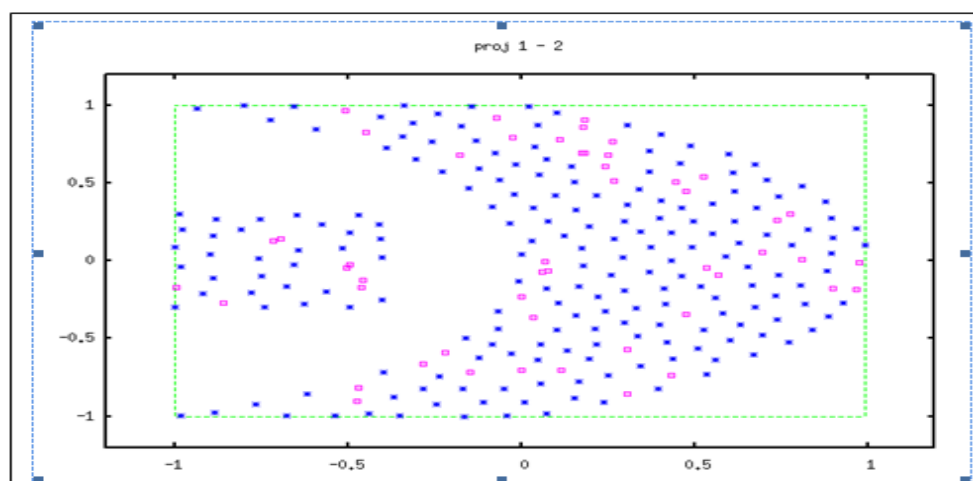
### 4.2 Optimal experiment design

All the modeling approach needs experimentation that could have high cost and users want to efficiently choose which experimentations those have to be done. Some optimal experiment design (OED) can be combined with modeling approach to design efficiently the experimentation database. The term efficient could have different meaning depending on which OED we focus on. In general for a given confidence level on the model, the designer wants to minimize the number of experimentation.

The optimized samples in the experimentation database could be just elaborated from physical knowledge<sup>6</sup> and in some techniques more optimized when model prototype is given. In some modeling technique (such as design of experiment) the whole given database is necessary to elaborate model and depend of model prototype and in other more flexible approaches the database is just suggested and not necessarily optimized for one model prototype.

### 4.3 Generating new experiments

User only needs to specify their input parameters and ranges of variation. InputSampler will manage samples generation by guaranteeing a best distribution of your samples in N-dimension. Figure 20 shows how input sampler generates new samples (red points) based on precedent ones (blue points) by regularly distributing them in multi-dimensions space.

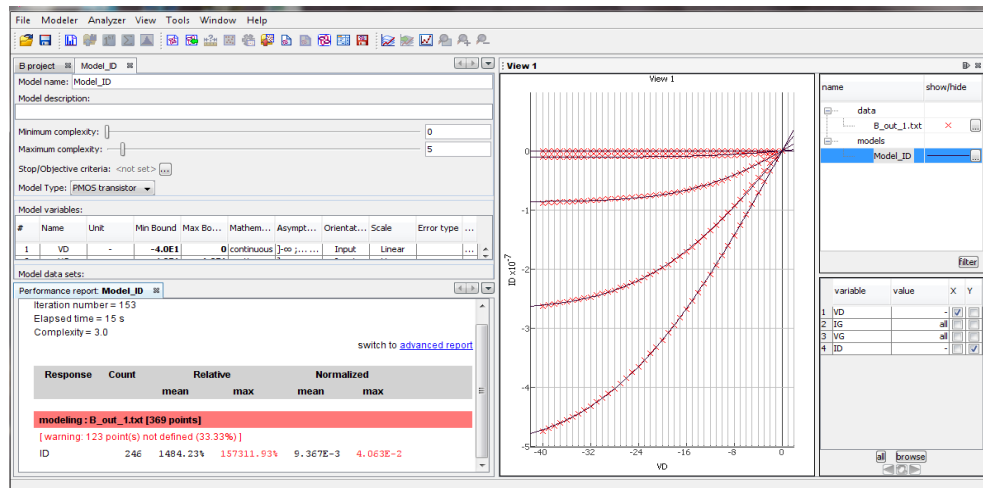


**Figure 20: Incremental input sampler.**

<sup>6</sup> in most of the case the role of physics knowledge consist of defining and/or limiting the parameter space domain of interest and specifying experimentation protocols

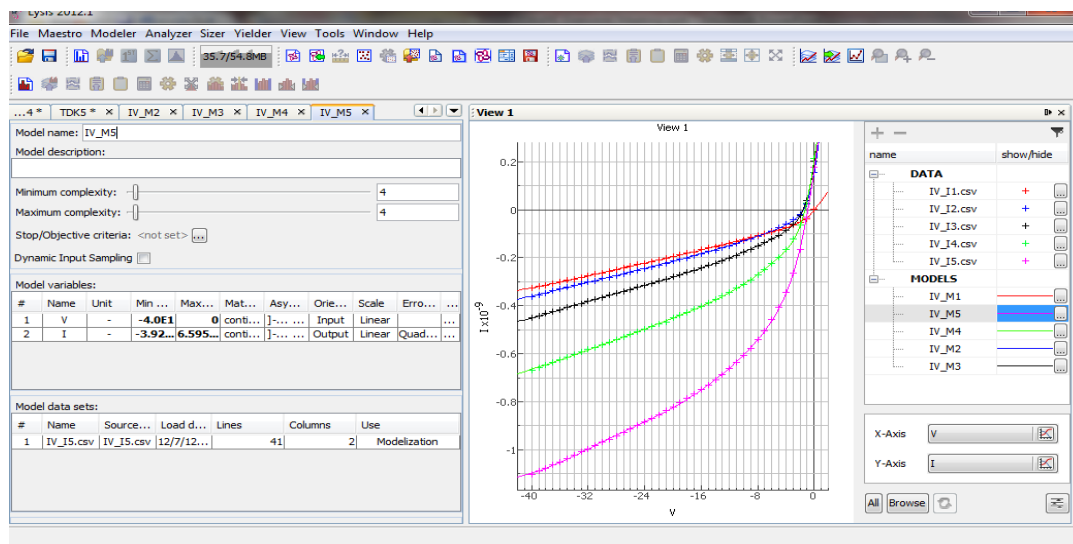
Please note that input sampler can be very efficient for validation. As it guarantees a good distribution of the new generated samples depending on the existing ones, these new samples can be used to validate the models in an external validation.

Based on data provided by ENEA on the fabricated OTFTs, the results of modeling are shown in Figure 21.



**Figure 21: Modeling ENEA OTFT**

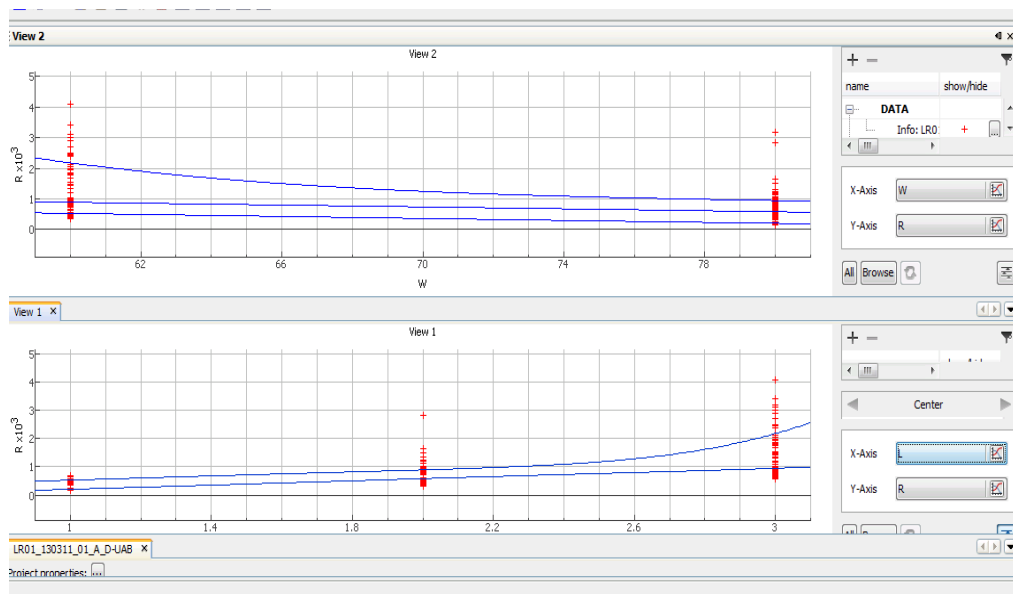
The same data have been used for the semi-physical modeling method (Figure 22). Fitting seems to be very good between measurements and the resulting analytical model. This model has been exported into Verilog-A format in order to use into spice simulators.



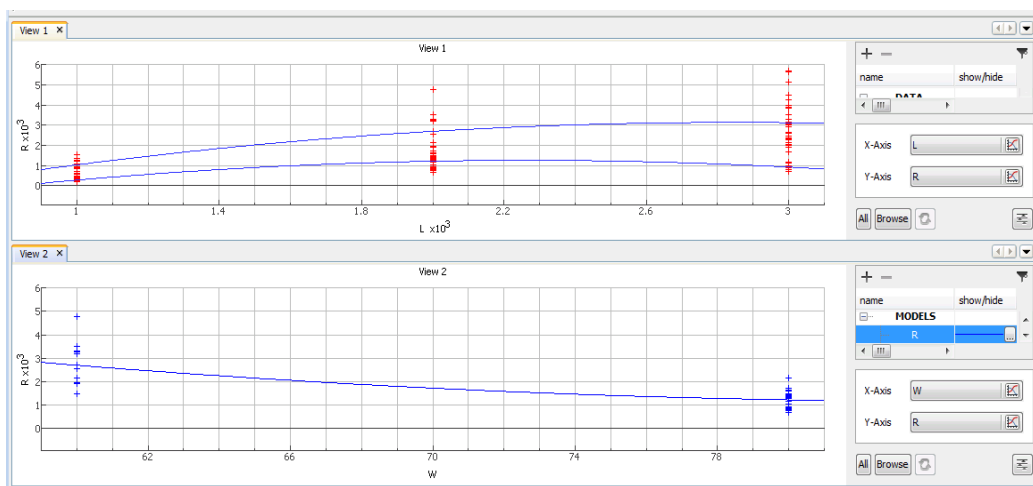
**Figure 22: Semi-Physical modeling of OTFTs data.**

### 4.4 Modeling trial of the horizontal linear resistor LR01

Modeling shows  $R$  as function of  $L$  and  $W$  (curves in blue) where red points are the measurements. However, printing variations make that even if we intend to print the same dimensions, variability impacts the printed resistors.



**Figure 23: Variability curves for LR01\_A\_130405\_01\_D-UAB\_130423**



**Figure 24: Variability curves for LR02\_130321\_01\_A\_D-UAB**

## 5 Validation

### 5.1 Blind validation

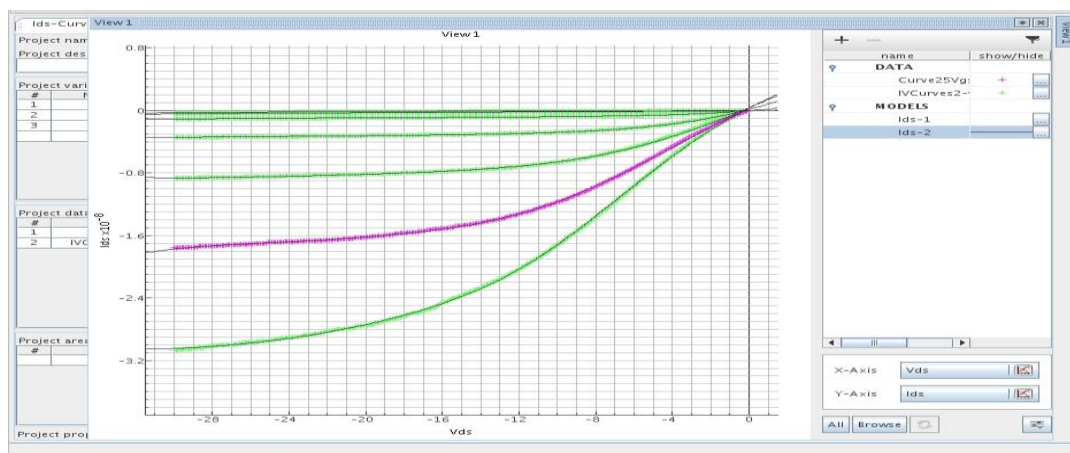
Data set (measurements) are divided into two subsets: one for modeling and the other for validation. The first subset, the modeling data, is used to fit the phenomena. The modeling process does not see the validation data. The second subset is then used only for validation. Generally, validation data subset size should be 10 to 20% of the whole data set.

Through modeling operation, an error report is displayed showing errors on the 2 subsets. This report includes global mean and maximum error (for different kind of errors) and more detailed error statistics for each loaded datasets and each output variable of the model.

After modeling a model performance report of computed model can be obtained.

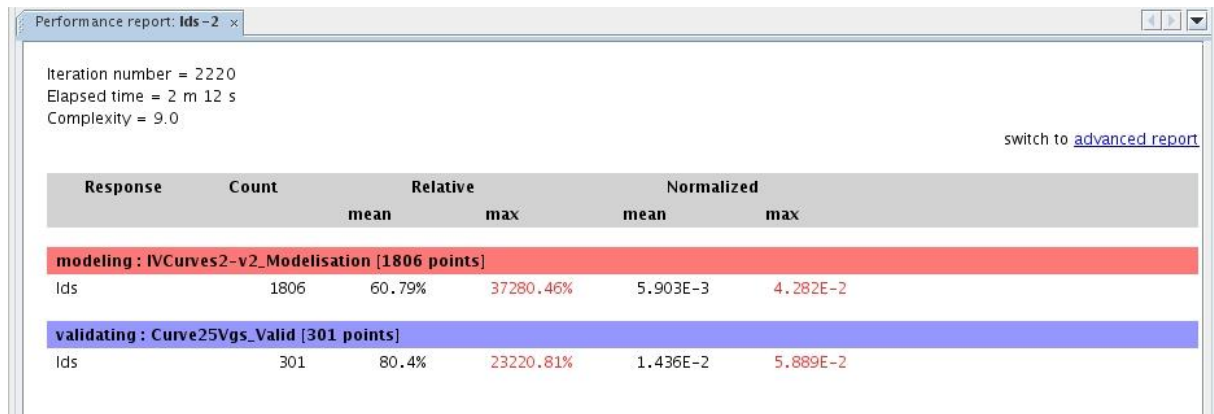
This report describes modeling error for different kind of error (quadratic, relative and normalized error) and for the different data sets and areas of data. This report contains a summary of mean and maximum error for each data set, areas and each output variables.

The following figure (Figure 25) shows that the modeling data in green and the validation one in red. Red curve is not seen by the modeling process.



**Figure 25: Semi-Physical modeling of OTFTs data.**

The following snapshot (Figure 26) shows in red the error report on modeling data and in blue the errors on validation data. One can see the relative and the normalized errors on the modeling (green curves) and validation (red curve).



**Figure 26: Error report on modeling and validation data.**

## 5.2 Viewing models behavior

At first validation level the physician can view the new created models. He will be able to see if curves represent what he was expecting from his knowledge of the physical phenomena.

## 5.3 Validation based on new printed samples

Once models are generated, they can be used for extrapolation. New samples can be generated (thanks to the input sampler) and the models are called to provide their performances.

These samples can be printed and then comparison can be done between model-based performances and lab measurements.

## **6 Model validity**

The model is valid in the range extracted from the given data. The model is guaranteed within this range. However, the Input Sampler can be used to generate samples within given ranges for all parameters. Input Sampler generates optimized data base and enable the modeler to create validated models on these ranges. The input sampler has many advantages as optimizing the needed samples, better coverage and better validation.

### **6.1 Models export**

Models are exported in various formats such as c-coded program or Verilog-A.

## 7 Dynamic modeling

INFINISCALE will develop templates for each device in order to integrate dynamic behavior to generated models. The model that has been already delivered in Verilog-A format was integrating the dynamic. So when exporting the models, the dynamic is automatically added.

The strategy is to have a template for each device.

Here after is a sample of an already delivered Verilog-A model.

```
`include "disciplines.h"
module tm_trans_pmos_id(D,G,S);

`include "tm_ids_curve2_ids_function.v"

inout D, G, S;
electrical D, G, S;
real id;
real vd, vg;

analog begin

    vd = V(D,S);
    if (vd > 0) begin
        vg = V(G,D);
        vd = V(S,D);
        id = -tm_vlg_ids_curve2_ids(vd, vg);
    end
    else begin
        vg = V(G,S);
        vd = V(D,S);
        id = tm_vlg_ids_curve2_ids(vd, vg);
    end

    I(D,S) <+ id;
end
endmodule
```

[VERILOG-AMS Module]  
NAME = tm\_trans\_pmos\_id  
SOURCE = tm\_trans\_pmos\_id.va

[Ports]  
(PORT TERMINAL D INOUT  
electrical )  
(PORT TERMINAL G INOUT  
electrical )  
(PORT TERMINAL S INOUT  
electrical )

[Declarations]  
[...]  
NCH D,S )  
NCH G,D )  
NCH G,S )

```
analog function real
tm_vlg_ids_curve2_ids;
input Vds;
real Vds;
input Vgs;
real Vgs;

[...]  
begin  
[...]  
x17 = (-2.4929409568106327E-9) +  
(x16) * (3.0588790784003937E-9);

tm_vlg_ids_curve2_ids = x17;

end

endfunction
```



## 8 Variability

Having defined the parameters and their extraction procedure, large number of measurements will be carried out to quantify variability. The statistical distribution of each parameter is then provided to the simulation models described above.

Variability in OTFTs is more acute than in silicon-based technologies by an inherently much higher parameter spread. Reasons for that, include, irregular morphology of the semiconductor, difficulty in controlling the precise dimensions of OTFTs, immobile trapped charges in the dielectric, uneven material deposition, roughness of the semiconductor-gate dielectric interface which leads to mobility variations between the different transistors.

Furthermore, it is important to have in mind that  $I$ - $V$  characteristics of OTFTs are known to change with the application of prolonged voltages, i.e. bias-stress effect, which leads to operational instability. This means that measurements procedures can introduce extrinsic variability on the OTFT parameter. ( $V_T$  may depend on the history, of the device, ambient light and setting parameters to record the OTFT electrical characteristics)

Accurate and efficient characterization of the different types of variation requires a large number of measurements on a variety of devices, layout styles, and environments. Most important it also requires:

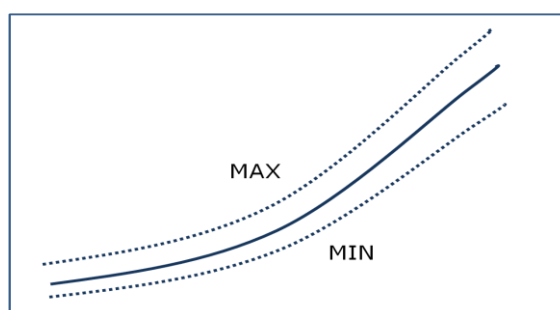
1. A physical model that can unambiguously define the parameters to be extracted.
2. A fixed and harmonized procedure for parameter extraction that minimizes extrinsic causes for variability.

### 8.1 Variability Management

#### 8.1.1 Variability management on mathematical models

INFINISCALE modeling is able to take into account the measurement variability. To consider variability in this case, this could be done in different ways:

1. Modelize a kind of envelope that delimits the variability range of each model (Figure 27)



**Figure 27: Managing Variability by MIN/MAX modeling.**

2. Or to add statistical distributions of technological parameters. In this case, many measurements should be repeated on the same device to capture variations.

### 8.1.2 Variability management on physical models

Physical models should represent variability. Here after some examples, extracted from a free 45n DK, showing how variability is expressed:

```

** FREE PTM 45nm MOS Library
** GLOBAL Variability

.LIB PTM45_STAT
.PARAM NTOXP_CMOS045 = AGAUSS(0.0, 1.0)
.PARAM NTOXM_CMOS045 = AGAUSS(0.0, 1.0)
...
// NTOXP_CMOS045 is define as a Gaussian distribution with 0 as mean and sigma =1
// NTOXM_CMOS045 is define as a Gaussian distribution with 0 as mean and sigma =1
.LIB "ptm45.lib" PTM45_EQ
.LIB "ptm45.lib" PTM45_MODEL
.ENDL

.LIB PTM45_EQ
.PARAM NMOS_TOXP = '1.10e-09 + 5.0e-11 * NTOXP_CMOS045'
.PARAM NMOS_TOXM = '1.75e-09 + 5.0e-11 * NTOXM_CMOS045'
...
.ENDL

** LOCAL Variability
.LIB PTM45_MODEL
.SUBCKT NPTM45 D G S B
+      W=50 L=50 MULT=1
.PARAM TOXE_CMOS0451 = AGAUSS(0.0, 1.0)
// TOXE-CMOS0451 is define as a Gaussian distribution with 0 as mean and sigma =1

.PARAM NMOS_TOXE = '1.75e-09 + 5.0e-11 * TOXE_CMOS0451'

.PARAM TOMETER = 1.0e-9

.PARAM XL = 'L * TOMETER'
.PARAM XW = 'W * TOMETER'

M1 D G S B NMOS W='XW' L='XL' M='MULT'

.model NMOS nmos level = 54
.....

* parameters customized by the user
+toxe = 'NMOS_TOXE'      toxp = NMOS_TOXP      toxm = NMOS_TOXM      toxref = 1.75e-09
+dtox = 6.5e-10      lint = 3.75e-09
...

.ENDS

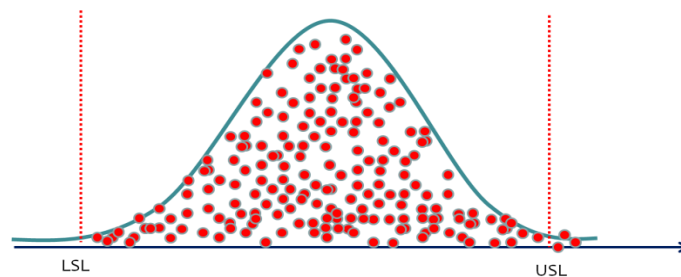
```

Statistical distributions are used by the spice simulator Monte Carlo (MC) analysis to achieve different simulations by picking up for each parameter (defined with statistical distribution) a new value following its PDF (Probability Density function).

The Monte Carlo procedure is the following:

1. Define inputs as probability distributions
2. Generate inputs values as randomly from a [probability distribution](#).
3. For each inputs vector (which is [deterministic](#)) perform the computation
4. The operation is repeated depending the number of required MC runs

Statistically talking, the number of MC runs should be big enough in order to guarantee acceptable accuracy.



**Figure 28: Monte Carlo sampling.**

## 8.2 Strategy to cope with variability and yield

The basic idea to cope variability is to introduce additional parameters to model what could explain the diverse variability effects. These additional parameters will be of 2 forms:

(a) Physical parameters. The values of these parameters will be extracted from the measurement curves. Their probability density functions (pdf) will be estimated from these data. The pdf estimation parameter will be simple Gaussian/uniform distribution or based on a weighted sum of Gaussian/uniform distributions.

(b) Mathematical parameters. These parameters will be pure mathematical variables that help to reduce residual error between model (without variability) and measurement data. The pdf will also be estimated from this residual error.

### 8.2.1 One model per transistor dimension

The current inkjet process developed in our project, has still a limited yield. This forced us to take a strategy oriented to optimize the yield by restricting the size of the transistors to those that show better yield often related to better morphological results (according to coffee ring effects, etc.).

This lets to the use of a limited number of transistors dimensions. This strategy is even best suited for the inherent regularity of the Inkjet Gate Array architecture, and let us to look for models in which W and L are fixed parameters.

In this case, statistical analysis will manage inherent variability to provide the physical and/or mathematical parameters.

For Infiniscale semi-physical model (see section 9.1.1), additional parameters are already supported by the tool, and the tool will provide VerilogA models for the transistor current in the form  $I(V_T, V_G, X_1, X_2, \dots)$  where  $X_1, X_2, \dots$  are additional physical or mathematical parameters.

For UCM physical model, the additional physical parameters are already incorporated, and the mathematical parameters will be added in the equation when there is a lack of accuracy of the model. Then, this new equation will be edited and optimized in the modeller tool presented previously.

### **8.2.2 General model for OTFTs**

For a general model integrating the dependency on transistor dimensions, the process parameter of form (b) must be carefully defined to be pertinent for all the various dimension of the transistors.

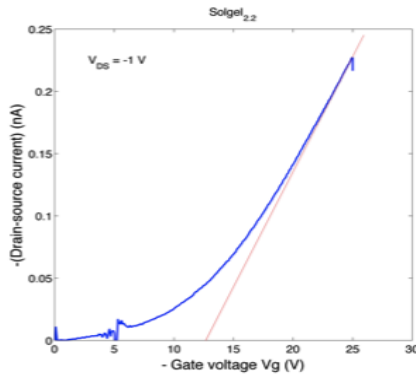
Then, for Infiniscale semi-physical model, the length/width will be considered as parameter in the tool (as in section 8.2.1) and the behavioral modeling tool will automatically link these new variables with output data.

For UCM physical model, we need to consider the interaction (if any) of transistor dimension and parameter of form (b) in the equation. And thus the impact of dimension on residual error between model (without variability) and measurement data must be carefully studied.

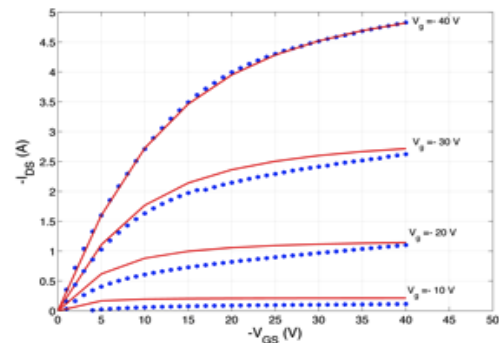
## **8.3 Variability analysis**

### **8.3.1 Preliminary example of the application of the UMEM model to simulates I-V characteristics of OTFTs produced within the TDK4PE consortium**

Figure 29 shows a transfer curve of typical OFET fabricated and characterized by the TDK4PE consortium. The OFET uses a solgel dielectric layer provided by Sun Chemical and as active semiconducting layer a blend of a soluble small molecule organic semiconductor and a polymeric additive designed to control the crystallization of the semiconductor upon film formation. This blend is named FS 0013 and is provided by Flexink. The transfer curve was measured in the linear region. In contrast to a trap-free OTFT the curve is not linear as expected. Therefore, neither the mobility ( $\mu$ ) neither the threshold voltage ( $V_{th}$ ) can be unambiguously determined.



**Figure 29: Transfer curve measured in the liner region ( $V_{DS} = -1V$ )**



**Figure 30: Comparison between experimental (dotted line) and simulated (full line) I-V characteristics using the UMEM model**

The fact that transfer curve is not linear is taken into account by the UMEM model through a parameter  $\gamma$ . Gamma ( $\gamma$ ) is a parameter that takes into account how far the OFET deviates from a trap-free OFET. The non-linear behavior is due to the presence of traps.

The output characteristics also suffer from "contact effects" as explained previously these effects can be taken into account by adding a voltage dependent contact resistance. These effects have not been considered in this particular fit, for this reason the fitting is not perfect for all the curves. TFT parameters extracted from the simulation of the output I-V curves are shown in Table 6.

TFT parameters		
$\mu$	$\gamma$	( $V_{th}$ )
$1 \times 10^{-4}$ ( $\text{cm}^2/\text{Vs}$ )	0.9	-2.55 (V)

**Table 6. TFT parameters extracted from the simulation of the output I-V curves**

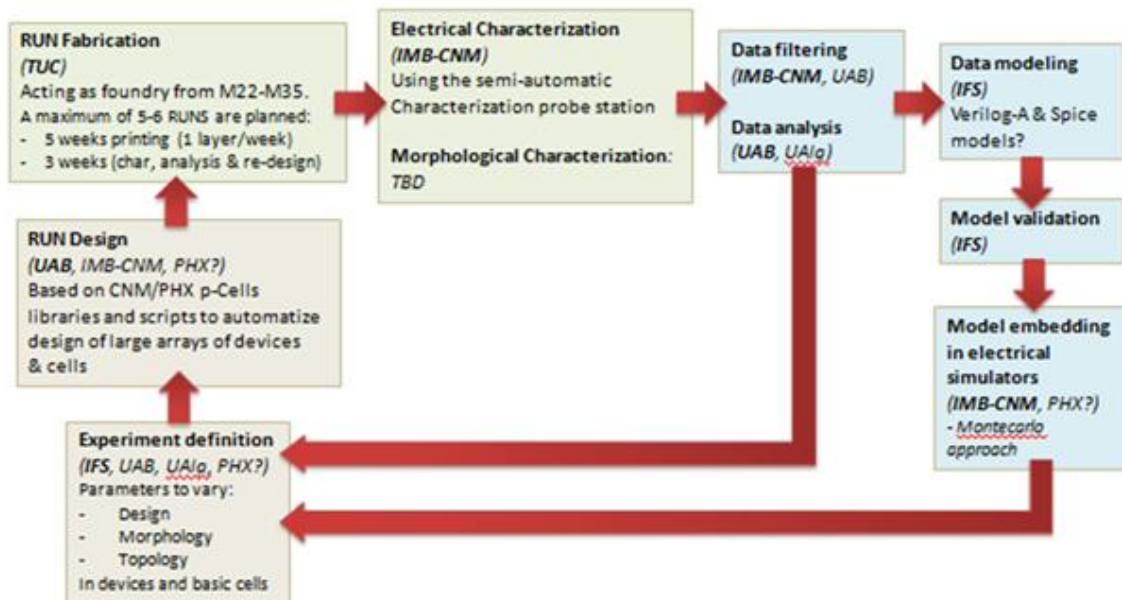
Physical parameters used are  $W/L=1000/30$ ,  $t_{ox} = 1 \mu\text{m}$ ,  $C_{ox} = 2.3\text{nF}/\text{cm}^2$ . The OFET was fabricated using printed layer of a solgel dielectric and FS 0013 as a semiconductor.

## 9 Methodology proposed inside TDK4PE

Variability and design verification could be done by Pre-defined Corners (PDC). However, PDC proved to be no more sufficient for new nanometer nodes for silicon electronics where number of impacting parameters became huge and physical impact became highly non linear. This is exactly why Monte Carlo analysis has emerged as a suitable technique for variability treatment. But, MC analysis is time consuming especially for long-simulated designs, which pushed for the need to new MC analysis as Fast Monte Carlo recently introduced.

Anyway, both techniques could be studied within TDK4PE and the most suitable will be selected.

The next schema shows the involved groups and their responsibilities for variability management taking into account all the steps of the chain and the different WP activities.



**Figure 31: Managing variability within the consortium**

### 9.1 Integrated models

#### 9.1.1 Infiniscale Semi-physical model

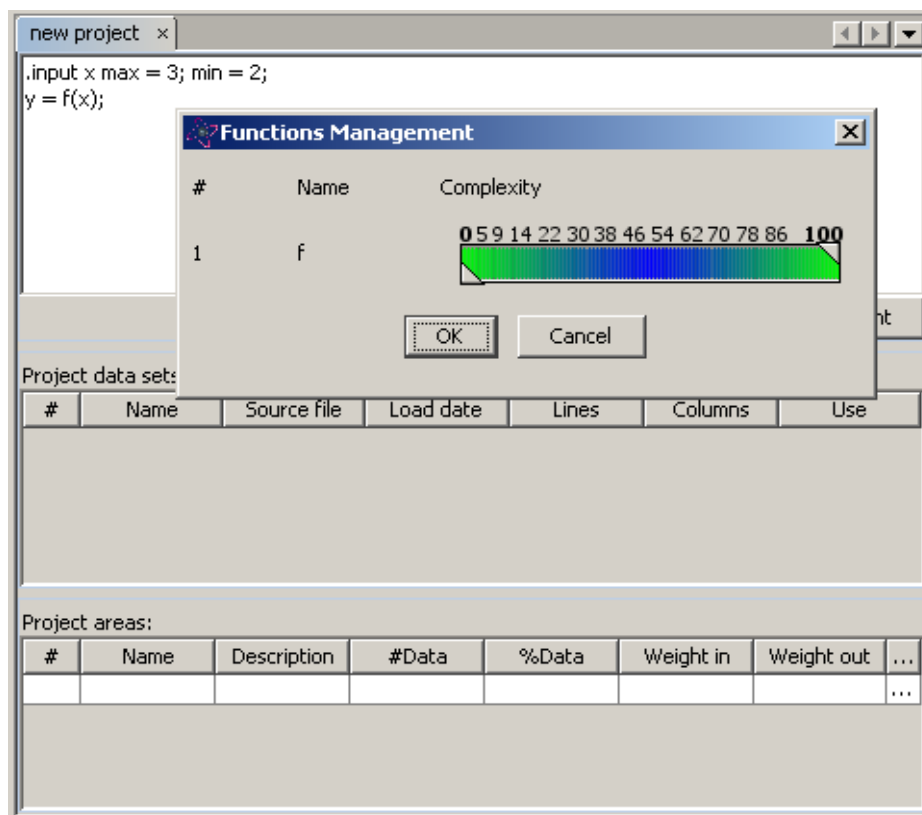
What is called Infiniscale semi-physical modeling is based on mathematical function plus information that physician can provide to guarantee that the generated model respect physical aspects.

To be noted that this model doesn't provide mobility or threshold voltage information, only the drain current as a function of drain and gate voltages (and potentially other parameters, if provided, as for example length, width of transistors, ...).

The "physical" information/constraints integrated in these models concern (mainly) the monotony, asymptotic behavior, cross of zero of the curves but not physical parameter (that are used in common physical model). Note that this drain current function (compiled in verilog-A) is sufficient to simulate the circuit [17].

### 9.1.2 UCM Semi-physical model

Infiniscale's extractor is in progress (figure 36) and new capabilities have been added to the parse. Infiniscale team is also working on the integration of UCM models. It is expected that Infiniscale will be able to deliver new models based on UCM models during December 2013.



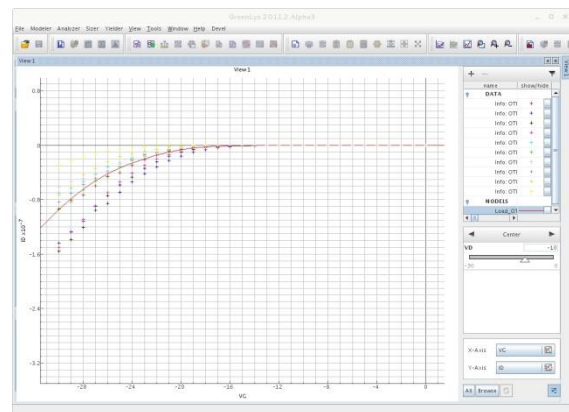
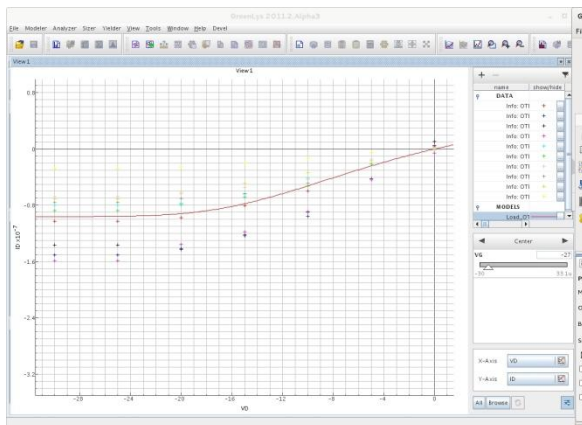
**Figure 32: New semi-physical GUI**

## 9.2 Example Devices

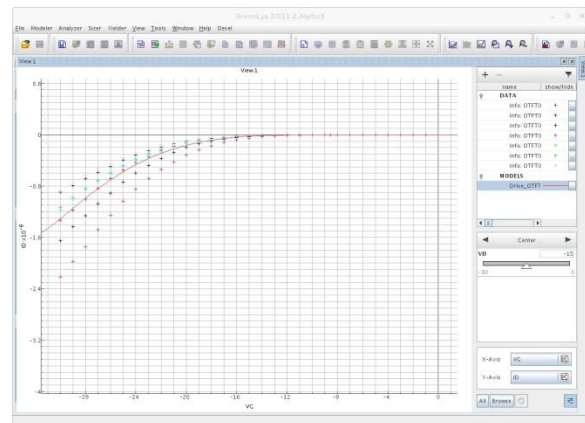
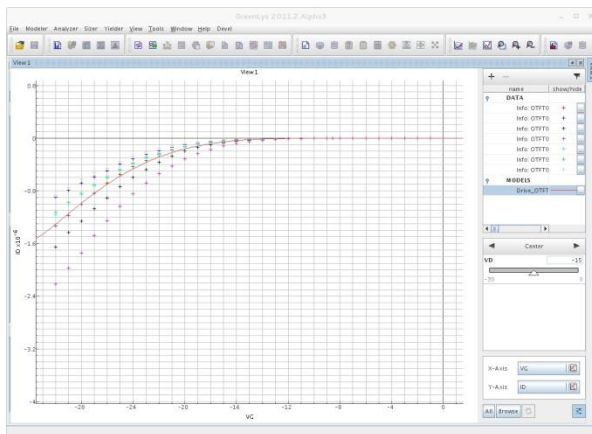
### 9.2.1 Load and Drive OTFTs

Two models for load (Figure 33) and drive (Figure 34) OTFTs have been generated. Load and drive names correspond to current pseudo-PMOS cell design style naming. Models are ID(VD, VG) were range of VD and VG are between [-30V, 0V]. Models were exported to verilogA for spice simulation purposes.





**Figure 33: Load OTFT: ID-vs-VD and Load OTFT ID vs VG**



**Figure 34: Drive OTFT modeling: ID vs VD and ID vs VG**

## 9.3 Example Circuits

### 9.3.1 Inverters and Ring Oscillator

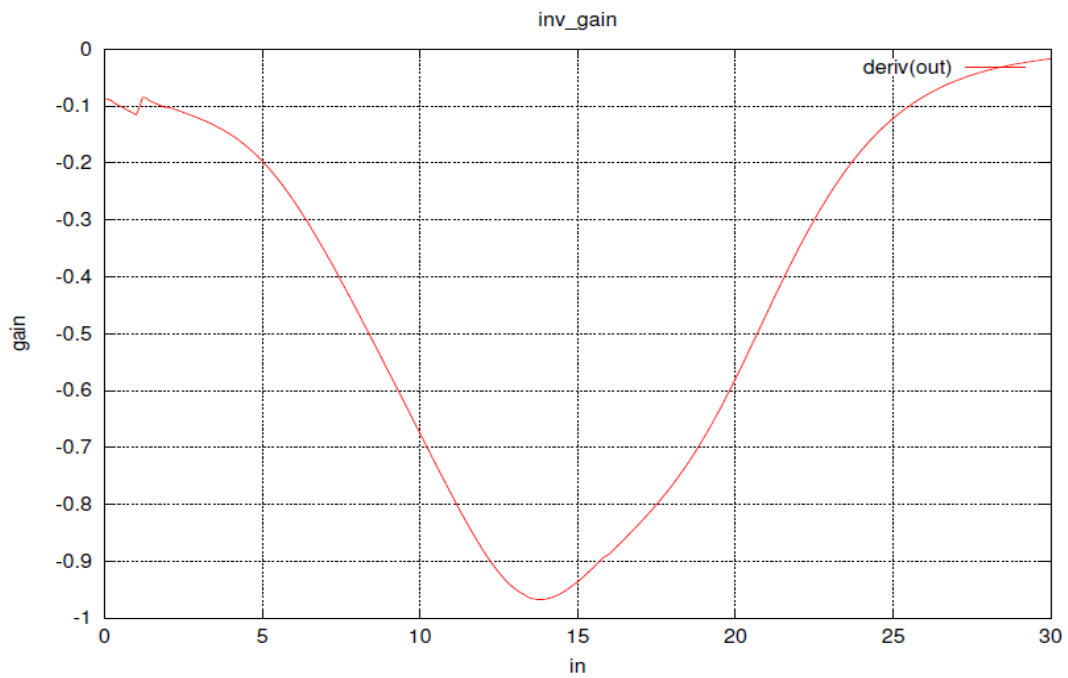
A three-step ring oscillator using the latest models provided by Infiniscale has been simulated. However, good results could not be obtained.

Inspecting the inverters made using the 'drive' and 'load' transistor models, a quite poor performance for the transfer curve has been observed due to the low transistor transconductance.

Attached you can find two graph (figure 39) showing the inverter transfer curve (look at the poor '0'), and its derivative (i.e. the gain). Since the gain is not reaching -1, no ring oscillator can be made, and it will be difficult to construct logical gates using this structures.

However, we could close the loop for the first time.





**Figure 35: simulated inverter transfer curve based on semi-physical models**

## 10 Conclusions

This document clarifies the concepts and procedures concerning Modeling, Validation and Variability Management for the devices built inside the TDK4PE project, especially for Organic Thin Film Transistors.

Critical issues that clarify our approach are:

1. Separate: (i) the concept of statistical variability on the parameters measured for a given set of devices, from (ii) the concept of variation on the model parameters considering the results from the extraction-modeling tool.
2. Propose a model in which the corner or the Monte Carlo analysis can be implemented considering different variations for every single transistor. That is to say, since every transistor is different from each other, each transistor instance should pass to the OTFT transistor model a different parameter to reflect that different behavior. Then, INFINISCALE (IFS) will provide a solution to be compatible with the existing model cells and simulation engines.
3. Consider that we have a reduced set of OTFTs sizes in our circuits (those that can be produced with highest yield), so that there will be a reduced set of models (i.e. OTFT1cm or OTFT4cm) that will be used/called from the circuit structures. This means that, at this first stage, we are not going to have one model for all OTFTs considering channel width ( $W$ ) and channel length ( $L$ ) variations but a model for a reduced set of fixed  $W$  and  $L$  values that take into account their statistical fabrication variation. Variability should then refer to the working conditions (i.e. power supply,  $V_{DD}$ ,  $G_{ND}$ ,  $-V_{SS}$ ) and physical parameters (gamma, mobility, threshold voltage, etc.). A global general model can also be used if a wide range of working OTFTs is available with sufficient performance.

## 11 References

### 11.1 Documents

- [1] S.Smith, "Sheet Resistance and Electrical Linewidth test structure for semiconductor process characterization", M.S. thesis. Univ. of Edinburgh, 2003.
- [2] A.L.Walton "Microelectronic Test Structures", abstract presented to Semicon97, Geneva.
- [3] N.Stavitski, J.H.Klootwijk, H.W. van Zeijl, B.K. Boksteen, A.Y. Kovalgin, R.A.M. Wolters, "Cross-Bridge Kelvin Resistor (CBKR) Structures for Measurement of Low Contact Resistances", IEEE Transactions on Semiconductor Manufacturing, Vol. 22, n. 1, February 2009.
- [4] N.Stavitski, J.H.Klootwijk, H.W. van Zeijl, A.Y. Kovalgin, R.A.M. Wolters, "A study of Cross-Bridge Kelvin Resistor Structures for Reliable Measurement of Low Contact Resistances", 2008 IEEE Conference on Microelectronics Test Structures, March 24-27, Edinburgh, UK.
- [5] Mohan, S.S.; del Mar Hershenson, M.; Boyd, S.P.; Lee, T.H., "Simple accurate expressions for planar spiral inductances," Solid-State Circuits, IEEE Journal of, vol.34, no.10, pp.1419-1424, Oct 1999 doi: 10.1109/4.792620
- [6] "Agilent Impedance Measurement Handbook", Application Note 5950-3000, 4<sup>th</sup> Edition, Agilent Technologies, Inc., 2009
- [7] Hammerstad, E.O., "Equations for Microstrip Circuit Design," Microwave Conference, 1975. 5th European, vol., no., pp.268,272, 1-4 Sept. 1975, doi: 10.1109/EUMA.1975.332206
- [8] Pucel, Robert A.; Masse, D.J.; Hartwig, C.P., "Losses in Microstrip," Microwave Theory and Techniques, IEEE Transactions on, vol.16, no.6, pp.342,350, Jun 1968 doi: 10.1109/TMTT.1968.1126691
- [9] "De-embedding Techniques in Advanced Design System", Agilent Technologies S.L.
- [10] P.Stallinga, "Electrical Characterization of Organic Electronic Materials and Devices", Wiley .ISBN: 978-0-470-75009-4.
- [11] A. Cerdeira, M. Estrada, R. García, A. Ortiz-Conde, F.J. García Sanchez, "New Procedure for the extraction of basic a-Si:H TFT model parameters in the linear and saturation regions", Solid State Electronics 45 (2001) 1077.
- [12] M. Estrada, A. Cerdeira, I. Mejia, M. Avila, R. Picos, L.F. Marsal, J. Pallares and B. Iñiguez, **1**. Modeling the behavior of charge carrier mobility with temperature in thin-film polymeric transistors, Microelectronic Engineering 87 (2010) 2565-2570.
- [13] M. Estrada, I. Mejía, A. Cerdeira, J. Pallares, L.F. Marsab, B. Iñiguez, Stability of PMMA on P3HT PTFTs under stress, SSE 53 (2009) p 1063-1066.
- [14] M. Estrada, I. Mejia, A. Cerdeira, J. Pallares, L.F. Marsal, B. Iniguez, Mobility model for compact device modeling of OTFTs made with different materials, Solid-State Electronics 52 (2008) 787.

- [15] I. Mejia, M. Estrada, M. Avila, "Improved upper contacts PMMA on P3HT PTFTS using photolithographic processes", *Microelectronics Reliability*, 48, 11-12, 2008, 1795-1799.
- [16] M. Estrada, I. Mejia, A. Cerdeira, J. Pallares, L.F. Marsal, B. Iniguez, *Solid-State Electronics*, 52, (2008), 787-794.
- [17] S. Jacob et al. "Compact modeling for Flexible Organic and Large Area Electronics: a new fast and reliable method", *LOPE-C*, 31 May 2010 - 2 June 2010, Frankfurt